Turun yliopisto
University of Turku

GRAPHENE FROM GRAPHITE BY CHEMICAL AND PHYSICAL TECHNIQUES

Jussi Kauppila

TURUN YLIOPISTON JULKAISUJA – ANNALES UNIVERSITATIS TURKUENSIS
Sarja - ser. AI osa - tom. 500 | Astronomica - Chemica - Physica - Mathematica | Turku 2014

University of Turku

Faculty of Mathematics and Natural Sciences
Department of Chemistry

Supervised by

Professor Carita Kvarnström
Department of Chemistry
University of Turku
Turku, Finland

Professor Jukka Lukkari
Department of Chemistry
University of Turku
Turku, Finland

Reviewed by

Professor Marja Lajunen
Department of Chemistry
University of Oulu
Oulu, Finland

Docent Di Wei
Wolfson College
University of Cambridge
Cambridge, United Kingdom

Opponent

Professor Francesco Paolucci
Department of Chemistry – Giacomo Ciamician
University of Bologna
Bologna, Italy

The originality of this thesis has been checked in accordance with the University of Turku quality assurance system using the Turnitin OriginalityCheck service.

ISBN 978-951-29-5937-2 (PRINT)
ISBN 978-951-29-5938-9 (PDF)
ISSN 0082-7002
Painosalama Oy - Turku, Finland 2014

Preface

The experimental work of this Thesis was carried out in the Laboratory of Materials Chemistry and Chemical Analysis in the University of Turku mostly between 2010 and 2014. The main funding for my research has come from Graduate School in Materials Research (GSMR) which later merged together with National Doctoral Programme in Nanoscience (NGS-NANO). Other funding sources were Magnus Ehrnrooth foundation, Department of Chemistry (University of Turku) and University of Turku Graduate School (UTUGS). I want to thank all the mentioned funding sources for enabling me to fully focus on my research and writing this Thesis.

First of all, I want to express my gratitude to my supervisors Carita Kvarnström and Jukka Lukkari who have made my research possible in the first place and guiding me on my way through the Ph.D. studies. This Thesis and many of my publications would not have seen the light of the day without tremendous amount of guidance and work by Antti Viinikanoja, who has been co-authoring many publications, teaching me to use most of the equipment in our laboratory and guiding me countless times. A huge thanks belongs also to all the other co-authors, especially Pia Damlin and Tom Lindfors, as well as everybody in the laboratory for their scientific and mental support. For the latter, I need to thank Emilia Palo, Bhushan Gadgil and Riku Sundell. In addition I want to thank Bhushan Gadgil for the XRD measurements and Jukka Hassinen for the TGA data and invaluable help in particle size distribution estimations.

Special thanks to Mauri, Kari and Kirsi for keeping the machines ticking, ones and zeros in order and chemicals flowing. And thanks for Kaisa for helping me to navigate through the endless sea of university bureaucracy.

Finally I want to thank my family and my girlfriend Anniina for supporting me all the way through my Ph.D. studies.

Turku, November 2014

Jussi Kauppila

Table of Contents

List of Included Publications

I A. Viinikanoja, J. Kauppila, P. Damlin, E. Mäkilä, J. Leiro, T. Ääritalo, J. Lukkari, Interactions between Graphene sheets and ionic molecules used for the shear-assisted exfoliation of natural graphite, Carbon, 68 (2014) 195-209

II J. Kauppila, L. Lund, M. Salomäki, T. Laiho, J. Lukkari, Effective low temperature reduction of graphene oxide with vanadium(III), Journal of Materials Chemistry C, 2 (2014) 3602-3609

III A. Viinikanoja, Z. Wang, J. Kauppila, C. Kvarnström, Electrochemical reduction of graphene oxide and its in situ spectroelectrochemical characterization, Physical Chemistry Chemical Physics, 14 (2012) 14003-14009

IV J. Kauppila, P. Kunnas, P. Damlin, A. Viinikanoja, C. Kvarnström, Electrochemical reduction of graphene oxide films in aqueous and organic solutions, Electrochimica Acta, 89 (2013) 84-89

V A. Viinikanoja, J. Kauppila, P. Damlin, M. Suominen, C. Kvarnström, In situ FTIR and Raman spectroelectrochemical characterization of graphene oxide upon electrochemical reduction in organic solvents, *submitted manuscript*

Reproduced with the permission of the copyright holders.

Contribution of the Author

Paper I: The author did most of the experimental work, wrote parts of the first draft of the manuscript and finalised it together with co-authors.

Paper II: The author did the experimental work together with one of the co-authors, wrote the first draft of the manuscript and finalised it together with co-authors.

Paper III: The author did part of the experimental work and finalised the manuscript together with co-authors.

Paper IV: The author did most of the experimental work, wrote the first draft of the manuscript and finalised it together with co-authors.

Paper V: The author did most of the experimental work, wrote parts of the first draft of the manuscript and finalised it together with co-authors.

List of Other Publications

N. Shrestha, M.-A. Shahbazi, F. Araújo, H. Zhang, E. Mäkilä, J. Kauppila, B. Sarmento, J. Salonen, J. Hirvonen, H. A. Santos, Chitosan-modified porous silicon microparticles for enhanced permeability of insulin across intestinal cell monolayers, Biomaterials, 35 (2014) 7172-7179

E. Mäkilä, M. Ferreira, H. Kivelä, S.-M. Niemi, A. Correia, M.-A. Shahbazi, J. Kauppila, J. Hirvonen, H. A. Santos, J. Salonen, Confinement effects on drugs in thermally hydrocarbonized porous silicon, Langmuir, 30 (2014) 2198-2205

T. Lindfors, A. Österholm, J. Kauppila, M. Pesonen, Electrochemical reduction of graphene oxide in electrically conducting poly(3,4-ethylenedioxythiophene) composite films, Electrochimica Acta, 110 (2013) 428-436

T. Lindfors, A. Österholm, J. Kauppila, R. E. Gyurcsányi, Enhanced electron transfer in composite films of reduced graphene oxide and poly(N-methylaniline), Carbon, 63 (2013) 588-592

J. Hassinen, J. Kauppila, J. Leiro, A. Määttänen, P. Ihalainen, J. Peltonen, J. Lukkari, Low-cost reduced graphene oxide-based conductometric nitrogen dioxide-sensitive sensor on paper, Analytical and Bioanalytical Chemistry, 405 (2013) 3611-3617

A. Österholm, T. Lindfors, J. Kauppila, P. Damlin, C. Kvarnström, Electrochemical incorporation of graphene oxide into conducting polymer films, Electrochimica Acta 83 (2012) 463-470

M. Pesonen, H.S. Majumdar, J. Kauppila, J. Lukkari, R. Österbacka, Large-scale solution processable graphene-based thin film devices, MRS Online Proceedings Library 1407 (2012) mrsf11-1407-aa20-25

Abbreviations

AFM	Atomic force microscopy
AN	Acetonitrile
ATR	Attenuated total reflection
CV	Cyclic voltammetry
CVD	Chemical vapour deposition
EDX	Energy dispersive X-ray spectroscopy
EG	Expandable graphite
Fc/Fc^+	Ferrocene/Ferrocenium (redox couple)
FT	Fourier transformation
GO	Graphene oxide
IR	Infrared (spectroscopy)
PC	Propylene carbonate
RGO	Reduced graphene oxide
SAED	Selected area (electron) dispersion
SEIRAS	Surface enhanced infrared absorption spectroscopy
SEM	Scanning electron microscope
SERS	Surface enhanced Raman spectroscopy
TEM	Transmission electron microscopy
THF	Tetrahydrofuran
XPS	X-ray photoelectron spectroscopy
XRD	X-ray diffraction

Abstract

Graphene is a material with extraordinary properties. Its mechanical and electrical properties are unparalleled but the difficulties in its production are hindering its breakthrough in on applications. Graphene is a two-dimensional material made entirely of carbon atoms and it is only a single atom thick. In this work, properties of graphene and graphene based materials are described, together with their common preparation techniques and related challenges. This Thesis concentrates on the top-down techniques, in which natural graphite is used as a precursor for the graphene production. Graphite consists of graphene sheets, which are stacked together tightly. In the top-down techniques various physical or chemical routes are used to overcome the forces keeping the graphene sheets together, and many of them are described in the Thesis. The most common chemical method is the oxidisation of graphite with strong oxidants, which creates a water-soluble graphene oxide. The properties of graphene oxide differ significantly from pristine graphene and, therefore, graphene oxide is often reduced to form materials collectively known as reduced graphene oxide.

In the experimental part, the main focus is on the chemical and electrochemical reduction of graphene oxide. A novel chemical route using vanadium is introduced and compared to other common chemical graphene oxide reduction methods. A strong emphasis is placed on electrochemical reduction of graphene oxide in various solvents. Raman and infrared spectroscopy are both used in *in situ* spectroelectrochemistry to closely monitor the spectral changes during the reduction process. These in situ techniques allow the precise control over the reduction process and even small changes in the material can be detected.

Graphene and few layer graphene were also prepared using a physical force to separate these materials from graphite. Special adsorbate molecules in aqueous solutions, together with sonic treatment, produce stable dispersions of graphene and few layer graphene sheets in water. This mechanical exfoliation method damages the graphene sheets considerable less than the chemical methods, although it suffers from a lower yield.

Keywords: Graphene, graphene oxide, reduced graphene oxide, mechanical exfoliation, electrochemistry, spectroelectrochemistry

Tiivistelmä

Grafeeni on materiaali, jonka mekaaniset ja sähköiset ominaisuudet ovat vertaansa vailla. Toisaalta grafeenin valmistaminen on erittäin haasteellista, eikä grafeenia tai grafeenipohjaisia tuotteita ole yleisesti markkinoilla. Grafeeni koostuu puhtaasti hiiliatomeista, jotka muodostavat tasomaisen, yhden atomin paksuisen kuusirengas-verkon. Tämä väitöskirja pyrkii esittelemään grafeenin ja grafeeninkaltaisten materiaalien perusominaisuudet sekä niiden valmistusmenetelmiä. Lähtökohtana väitöskirjassa on ylhäältä-alas –menetelmät, joissa grafiitista pyritään irrottamaan yksittäisiä grafeenilevyjä erilaisilla tekniikoilla. Grafiitti on luonnollinen grafeenilähde, sillä grafiitti koostuu puhtaasti päällekkäin pinoutuneista grafeeneista. Ylhäältä-alas –menetelmissä grafeenilevyjen välistä sitoutumista pyritään heikentämään kemiallisin tai fysikaalisin menetelmin ja lopulta saamaan yksittäiset grafeenilevyt irti toisistaan. Väitöskirjassa tutustutaan muutamiin erilaisiin menetelmiin, joista suosituin on grafiitin hapettaminen grafeenioksidiksi. Voimakkaat hapettimet saavat rikottua grafeenin aromaattisen rakenteen liittäen erilaisia happiryhmiä grafeeniin. Näiden ryhmien ansiosta grafeenioksidi on vesiliukoinen, mutta myös sen muut ominaisuudet poikkeavat merkittävästi grafeenin ominaisuuksista. Tämän takia grafeenioksidi pyritään usein pelkistämään takaisin grafeeniksi, tai pikemminkin pelkistetyksi grafeenioksidiksi.

Kokeellisessa osiossa nimenomaan grafeenioksidin pelkistäminen kemiallisesti ja sähkökemiallisesti ovat pääosassa. Työssä havaittiin muun muassa että vanadiinia voidaan hyödyntää grafeenioksidin pelkistämisessä ja sitä verrattiin muihin tunnettuihin pelkistimiin. Kemiallisten pelkistimien lisäksi työssä panostettiin sähkökemialliseen grafeenioksidin pelkistykseen. Sähkökemiallisesti grafeenioksidi voidaan pelkistää kontrolloidusti ja pelkistys voidaan suorittaa niin vesiliuoksissa kuin orgaanisissa liuottimissa. *In situ* spektrosähkökemialliset mittaukset mahdollistivat erittäin tarkkojen spektroskooppisten muutosten seurantaan graeenioksidia pelkistettäessä. Työssä hyödynnettiin sekä Raman- että infrapunaspektroskopiaa yhdistettynä sähkökemiallisiin mittauksiin.

Lisäksi grafeenia ja muutaman kerroksen paksuisia grafeenilevyjä erotettiin grafiitista käyttäen vain mekaanisia menetelmiä. Mekaanisten menetelmien etuna kemiallisiin menetelmiin nähden on niiden pienempi aiheuttamien rakenteellisten muutosten merkittävästi alempi määrä. Työssä grafeenia irrotettiin grafiitista käyttäen apuna voimakasta ultraääntä ja pieniä pintamolekyylejä, jotka mahdollistavat grafiitista irronneiden grafeenilevyjen vesiliukoisuuden.

Avainsanat: Grafeeni, grafeenioksidi, pelkistetty grafeenioksidi, mekaaninen erottelu, sähkökemia, spektrosähkökemia

1. Introduction

1.1. About Graphene

Graphene, that futuristic material that could bring computer processors into the next level, enable the operation of space elevators and solar powered, transparent, lightweight, foldable displays and computers. While graphene could be used to fulfil these more or less science fiction dreams, it has not done it yet. The lack these applications made from this wonder material is because of the difficulties in preparing high quality graphene in large scale. The handling of this almost completely transparent nano-scale material has proven to be quite tricky, too. Due to the lack of a single superior graphene manufacturing and handling method, various novel methods and techniques or modifications of the existing ones are constantly introduced into the research on graphene. So far, graphene, and several of its modifications, have been used in several composite materials and in sensor applications. Also many proof-of-concept devices have been presented, including transistors, displays and solar cells.

Graphene is, by definition, “a single-atom-thick sheet of hexagonally arranged, sp^2-bonded carbon atoms that is not an integral part of a carbon material, but is freely suspended or adhered on a foreign substrate”.[1] The really liberal use of the term graphene in literature had led the editors of the journal Carbon to post this suggested definition as well as definitions for other terms used in graphene research to clarify the nomenclature. Based on that, thicker graphene type nanoparticles should be called few-layer (2-5 layers) or multi-layer graphene (up to 10 layers). In addition, the lateral size of graphene sheets should be described, e.g., as nanosheets or microsheets. Other graphene sub species include narrow long graphene (nano)ribbons and graphene quantum dots (formerly known as polyaromatic hydrocarbons or PAH-compounds). Graphene as a research field is a rapidly evolving and expanding activity, producing numerous new research articles every day. Some significant leaps have been made even during the five years of the work on this Thesis, as new techniques have been developed and many applications and some commercial prototypes created.

What is graphene really, then? For a chemist, graphene is an insoluble large aromatic hydrocarbon molecule with undefined lateral size. This structure can be exposed to certain types of chemical reactions to modify its structure but otherwise graphene is chemically boring. From the point of view of materials science or materials chemistry and, especially, materials physics, graphene is a wonderful material and its properties are highly dependent on, e.g., environment conditions, the number of stacked graphene layers, the lateral size of the sheets, and their crystallinity. Therefore, the above mentioned nomenclature is important.

Graphene consists of fused benzene rings and can vary in size from just a single or few rings up to an infinite sheet. Single sheets graphene can be produced with lateral dimensions from centimetre scale to meter scale [2], which can already be considered infinite for most purposes. This represents a very fast pace of development, remembering that the first graphene sheet was isolated just ten years ago (2004). On the other hand, graphene was a theoretical material for a long time before its actual physical discovery, and it was used to explain and calculate the structure and properties of graphite, graphite intercalation compounds, carbon nanotubes and fullerenes. Andre Geim and Konstantin Novoselov used a “tape method” to produce the first monolayer graphene in 2004.[3] The tape method is basically a mechanical peeling of graphite into thinner and thinner sheets using an adhesive tape. This procedure is repeated until a single layer of graphite, graphene, was left on the tape. Needless to say, this method has its limitations, especially in quantity of material obtained, but it is still probably the best method to produce the highest quality graphene.

The structure of graphene is very strong in the plane of the sheet, caused by the alteration of strong chemical single and double bonds between the carbon atoms. In fact, graphene was the strongest material known until the recent theoretical predictions of the even stronger carbyne structure[4], and graphene still is the strongest existing material. Graphene is a two dimensional sheet which has a 2D Young’s modulus of 342 Nm^{-1}, corresponding to a traditional 3D Young’s modulus of 1.0 TPa if the interlayer distance of graphene sheets in graphite is used for the thickness of a single graphene sheet.[5] In the same study, the breaking strength of graphene was measured to be 42 Nm^{-1}. These measured values that were obtained with an atomic force microscope –based nanoindentation technique are identical to the theoretically predicted values of the Young’s modulus. On the other hand, carbyne is a theoretical one dimensional carbon chain with alternating single and triple bonds with a predicted Young’s modulus of 32.7 TPa.[4] The strength of graphene is similar to carbon nanotubes, which can be viewed as rolled graphene, but slightly higher due to extra stress in nanotubes caused by tight rolling. While graphene is mechanically very strong it is also lightweight and flexible. Graphene can be rolled without any damage to the structure although the applied stress causes observable changes in its electrical properties.[6] The strong and flexible material is ideal for many applications on its own, if large enough sheets are available, but usually graphene sheets are just a few micrometres wide. Nevertheless, these graphene microsheets have been used to enhance mechanical strength of many polymeric films.[7] Polymer-graphene composites are not comparable by their properties to pure graphene but are superior to pure polymers. To achieve this kind of improvement, the right polymer to graphene ratio as well as suitable chemical bonding between the materials is required. Therefore, graphene is often chemically modified before mixing with polymers in order to enhance the interactions. For example, graphene oxide (GO) and reduced graphene oxide

(RGO), which are discussed in details later, are more common materials in composites than graphene itself. The mechanical strength of graphene is not its only remarkable property. Graphene's tight carbon network does not allow any gases to pass through it. Even hydrogen molecules cannot penetrate a graphene film. Therefore graphene and its modifications have been used, e.g., in rubber composites to prevent permeation of gases.

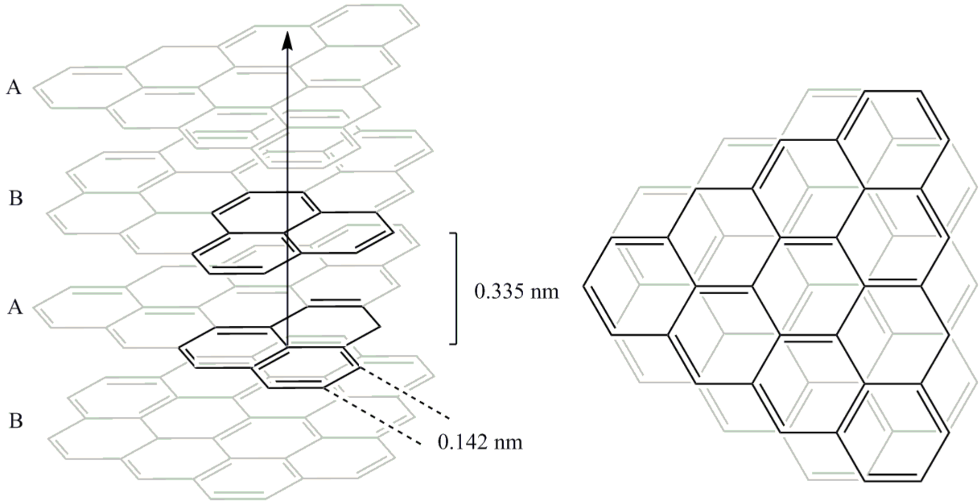

Figure 1. Structure of graphite showing the AB-stacked graphene sheets.

As mentioned earlier, a natural source for graphene is graphite. In fact, graphite is just a pile of graphene sheets. Usually graphene sheets are stacked neatly in an AB-stacking, where every other layer is positioned identically to each other (Fig. 1).[8] In graphite there are no chemical bonds between the individual graphene sheets. Due to the aromatic structure of graphene there is a π-electron network throughout the graphene sheet that interacts with the π-electrons of graphene sheets above and below. These π-π–interactions are quite weak but due to large surface area of the sheets the combined forces keep the individual sheets stacked to each other tightly, making their exfoliation difficult. On the other hand, because of the lack of strong chemical bonds between the sheets, they can quite easily slide with respect to each other. In fact, this property has been used in some graphite based lubricants.

In addition to its mechanical properties, the electrical properties of graphene are excellent. In conductive polymers an alternating single and double bond structure, called conjugated structure, enables the electrical charge to travel along the polymer chain. In the case of the graphene, the whole two dimensional material is constructed from alternating single and double bonds between carbon atoms. This creates a "frictionless" surface where electrons move freely, not just along one chain, but through the whole graphene sheet. In fact, the mobility of charge carriers in graphene is extremely good, 15000 $cm^2V^{-1}s^{-1}$, making electrons behave like massless Dirac fermions [9]. Despite this, graphene is a zero band gap semiconductor rather than a conductor. This means that at charge neutrality point, e.g. at undoped stage, graphene has zero conductivity. Any kind of a doping, either positive or negative, chemical or electrical, makes graphene conducting. At room temperature some conductivity is always observed due to thermal excitation of electron over the zero band gap. Therefore, graphene transistor can never be turned off. By manipulating the shape and size of graphene, or the number of graphene layers, a band gap can be created and the material used as a semiconductor, e.g., in transistors. Because there is no minimum gate voltage required to cause electrical current to flow through, graphene is easily affected by external factors. Due to graphene's sensibility to environment it can be used as a sensor material. When graphene is in contact with surface or charged molecules the electrical conductivity is affected. With transistors, an external gate voltage is applied to increase the current but in sensors the analyte molecules cause the change in conductivity.

While the lateral dimensions of graphene can be from few nanometres to infinity, the thickness of the graphene sheet is just the thickness of one carbon atom. Because doped graphene can have excellent conductivity, many optical electronic devices would only require very thin graphene films or even just one layer of graphene to achieve the desired properties. These types of thin films would be almost transparent as 97.7 % of the light in the visible range will travel through a single sheet of graphene.[10]

As graphene is slowly making its way out of laboratories into the commercial products it is important to consider its safety to humans and the environment. The safety or toxicity of graphene, and other graphene based materials, is a complicated matter without an easy and comprehensive answer. The main problems are the huge variety of graphene based materials and the lack of systematic studies on these materials. Because graphene is a single layer carbon sheet, it does not have definite lateral dimension and it may, in nature, restack into thicker structures. Dimension of the graphene is one of the most important parameter when regarding its toxicity. For example, smaller graphene sheets, in the cellular scale, might be phagocytised while larger graphene sheets cannot be dealt with by normal cell functions. To complicate thing even further, pure graphene has different physical, chemical and toxicological properties than modified graphene, including graphene oxide or reduced graphene oxide. While graphene itself is highly hydrophobic with a completely aromatic structure, graphene oxide has hardly any aromatic domains left in its structure and bears multiple oxygen containing functional groups, which make it hydrophilic. Reduced graphene oxide lies somewhere in between with fewer functional groups and greater aromatic domains than graphene oxide. In addition, an ever increasing number other chemical modifications, covalent and non-covalent, have been made to graphene materials in order to improve their properties. All these different modifications could affect the biological behaviour of the material. Much more information is needed about the possible toxicity of graphene based materials but something is already known and is summarised in a few recent reviews.[11-14] Based on this information, studies have so far indicated many possible mechanisms by which graphene based materials may harm biological subjects but many of these studies have focused on quite specific issues or used poorly controlled nanomaterial samples. The effect of graphene based materials on biological subjects is generally based on either the materials own chemical toxicity, a disrupted biological function or a direct physical damage to cells and tissues. Trace elements, such as manganese, or unintentional functional groups like amines, in the materials used increase their toxicity.

There are few different ways that humans can be exposed to graphene and its derivatives. Maybe the most probable and perhaps the most dangerous way, too, is through inhalation. Graphene is a very light material and when isolated as a single sheet or as a few layer graphene, it easily becomes airborne. Theoretical calculations have shown that graphene or few layer graphene with various sizes can reach at least the distal lung region.[12,15] The smaller sheets (~0.5 μm), especially, have no trouble of entering the distal lung but also bigger sheets (~25 μm) do it surprisingly well.[12] It still remains unclear how efficiently graphene sheets can find their way into the pleural space, but once there, experiments on mice have shown that few layer graphene can cause severe problems.[15] In another study, few layer graphene (or graphene aggregates) and polymer coated graphene were tested in mice by placing the particles in the lungs.[16] There they showed no direct toxicity but especially the graphene aggregates caused some fibrosis. GO, on the other hand, was shown in the same study, to be more acutely toxic than the other two tested materials. It seems that few layer graphene causes inflammation in lungs. This inflammation is at least partially caused by frustrated phagocytosis which is triggered by too massive sheets for phagocytes to handle. Another observed anomaly was the elevated level of reactive oxygen species. Unlike large graphene particles (< 15μm), small sheets up to 5 μm in diameter could be fully phagocytised[15], and small GO particles are fully phagocytised, too.[17] In all cases, the toxicity of graphene based materials is highly dependent on their physical and chemical nature. Hydrophilic graphene reacts more easily with cell walls than GO and do not easily enter the cells[17] but in blood circulation graphene, as a hydrophobic material, tends stay in the walls of veins while GO reacts aggressively with blood and forms aggregates which could lead to blood cloths.

Another possible human exposure routes, such as through the skin or through the digestive system, have not really received much attention. Finally, several graphene based sensor applications have been proposed, some of which could be positioned inside the human body. This opens up the possibility for “intentional exposure” for graphene. Regardless of the exposure route graphene based materials and applications should not be handled carelessly until further information about their safety is obtained.

1.2. Preparation of Graphene: the Bottom-Up and Top-Down Approaches

There are plenty of methods to produce graphene and graphene-like materials and new ways are continuously invented. The preparation methods can be divided in two categories: top-down and bottom-up –methods. Top-down methods intend to use natural or synthetic graphite and in various ways to peel off single graphene sheets from graphite. Bottom-up methods, on the other hand, usually make use small carbon containing molecules or some other carbon source and build up graphene structures by joining carbon atoms together to grow up graphene.

In the bottom-up category chemical vapour deposition (CVD) is the most used technique, since it can produce large area graphene sheets, with lateral dimensions up to several centimetres and with controlled number of graphene layers. CVD allows an easy control of layer thickness and coverage of large area and produces high quality graphene sheets. Two drawbacks of CVD are the requirement of a substrate with a matching surface crystallinity, which will enable graphene to build up properly, and the polycrystallinity of the produced graphene films. The polycrystalline structure is created when multiple small graphene islands are growing simultaneously on the substrate until they eventually merge together. As with most of polycrystalline materials, there are some defects at the crystal boundaries. These defects slightly hamper both the mechanical and electrical properties of graphene. Although the CVD-produced graphene films contain some defects they are very thin, have large lateral size, and are also relatively cheap to produce (in the world of graphene). For these reasons, the CVD graphene will most likely be the choice of electronics industry. For example, a sort of roll-to-roll CVD technique has been shown to produce graphene films with 30 inch (~76 cm) in diagonal length in 2010 [2] and 100 meter long rolls of CVD graphene in 2013 [18].

Another, but less a common bottom-up –method, is the polymerization of large aromatic hydrocarbons to larger graphene networks.[19] The dominant product of this method is, however, carbon nanoribbons and not graphene sheets. The most significant limitation of this technique is the decrease in solubility of products as the molecular size increases.

In this Thesis, the focus is on top-down methods, especially on the mechanical exfoliation of graphene and reduction of graphene oxide. In next chapters various methods for separating graphene sheets from graphite using mechanical and chemical methods are introduced.

1.3. Mechanical Methods for the Exfoliation of Natural Graphite

Mechanical methods for the preparation of graphene are based on applied mechanical forces that separate graphene sheets in graphite from each other. Additionally, these methods do not cause any chemical modification to graphene. Mechanical methods are especially desired when the highest possible quality is needed, e.g., in the investigation of the fundamental properties of graphene. The first method reported to produce graphene was a mechanical method called the *tape method* or *Scotch tape method*. The tape method yields low amounts of graphene sheets of high quality.[3] In its simplicity, the tape method works by placing graphite between two strips of tape and peeling graphite into thinner and thinner layers with the tape. After transferring the so-formed few and single layer sheets to a substrate, the latter sheets must be manually searched on the substrate. This method is highly inefficient but the formed graphene sheets are nearly flawless.

Removing graphene sheets from graphite requires quite strong forces. Paton et al. demonstrated that shear rates of 10^4 s^{-1} or higher are required to separate the sheets.[20] This rate is normally achieved with powerful mixers or ultrasonicators. As already mentioned, graphite consists mostly of AB stacked graphene sheets with a 3.34 Å spacing between the sheets although some ABC stacking pattern might also occur. In this structure, there are small “vacancies”, or intercalation sites, where small molecules, or more often ions like lithium, can be placed. Intercalated graphite has larger interlayer distance than pure graphite and, therefore, the force required to separate graphene sheets is lower. These kinds of materials are called graphite intercalation compounds. Graphite intercalation compounds could be used to produce graphene although not many studies have been published.[21]

Another type of intercalated graphite material is expandable graphite (EG). This material, which is also commercially available, is loaded with nitric or sulphuric acid. Like the metal ions also the intercalated acids push the graphene sheets a bit further away from each other making their exfoliation slightly easier compared to exfoliation in natural graphite. EG can be used as a starting material in various graphene production methods, including graphene oxide synthesis or in mechanical exfoliation. Expandable graphite can be thermally treated to produce expanded graphite with the volume that may be hundered times larger than the original. During rapid heating, the intercalated acids instantly vaporise and cause the material to undergo enormous expansion. While this method creates plenty of graphenes and few–layer graphene sheets, together with larger graphite pieces, it also damages the graphene sheets. First of all, the oxidising intercalated acids produce chemical changes, i.e., oxidation, of the graphene sheets and, secondly, the rapid thermal treatment causes physical damage to the sheets.

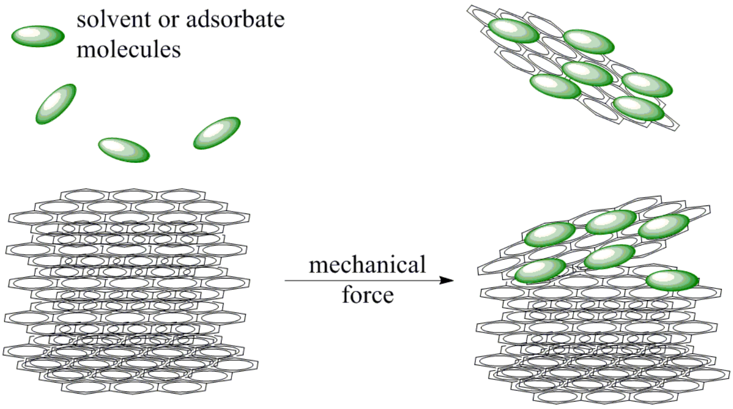

Figure 2. Exfoliation of graphene using adsorbates and mechanical force.

Liquid exfoliation techniques intent to get graphene exfoliated directly into solvents or solutions. Graphene is a hydrophobic material and, therefore, not soluble in water or any polar solvents in any significant concentrations. Furthermore, the graphene sheets are tightly attached to each other making them directly insoluble in any solvent. It was, however, discovered that small amounts of graphene could be dispersed in some organic solvents by using ultrasound.[22] Usually the amount of dispersed graphene sheets is less than 0.01 mg/ml and the exfoliated material consists of mainly mono and few layer graphene sheets with diameters usually less than a micrometre. In direct exfoliation of graphene in organic solvents it was noticed that the properties of solvent are crucial for graphene exfoliation. Initially, Coleman et al. tried to match the surface free energies of the solvents and graphene.[22] This work suggested that successful solvents should have surface tension between 40 and 50 mJm^{-2}. These values correspond, for example, to 1-methyl-2-pyrrolidinone, γ-butyrolactone and benzyl benzoate, which they found to be good solvents for graphene. Later, after analysing the solubility of graphene in forty different solvents, Coleman et al. noticed that the use of the Hansen solubility parameters led to a better match to their experimental results.[23] Hansen solubility parameters take into account the dispersion forces, dipolar intermolecular forces and hydrogen bonds between the solvent and graphene. In a recent review, Texter criticised the early *matching the surface energies* –approach advocated by Coleman et al.[22] and some others, stating that the theoretically correct approach should rather focus on minimising the interfacial energy between graphene and solvent.[24] He also critically reviewed other approaches including the use of Hildebrand and Hansen solubility parameters, which are often thermodynamically inaccurate, and would rather rely on molecular dynamics. While detailed understanding of the stability and solubility of graphene in various solvents is important, the choice of an optimal solvent is only one factor that affects the concentration and properties of the graphene solutions.

In order to increase the generally low graphene concentration, Khan et al. tested various sonication times, up to 460 h, for graphite in *N*-methyl-pyrrolidone. After 270 h of sonication they reached the maximum concentration of 1.2 mg/ml.[25] Another approach was used by Bourlinos et al. who used fluorinated aromatic solvents and achieved graphene concentrations up to 0.1 mg/ml.[26] In the same study, they also used various aromatic and ionic organic solvents and achieved concentrations in the range of 0.2-0.3 mg/ml, and as high as 1 mg/ml by using benzylamine. Since then, higher and higher concentration of few and single layer graphene have been dispersed in various solvents. Probably the highest concentration achieved by simply sonicating a graphite powder in organic solvent is 8.0 mg/ml of graphene in 3-glycidoxypropyl trimethoxysilane.[27] Recently it was shown, that by concentrating a dilute graphene solution, momentary concentrations up to 63 mg/ml and stable concentration of approximately 27 mg/ml could be achieved in *N*-methyl-pyrrolidone.[28] This was achieved by concentrating an initial graphene dispersion of 2.0 mg/ml by centrifugation and sonication. High concentration of few layer dispersed graphene makes easier its use in many applications, such as in conductive inks and composite fillers. Therefore, liquid-exfoliated graphene is an important alternative to GO based materials, which routinely achieve concentrations over 1 mg/ml. Many of the suitable solvents for liquid exfoliation, however, have a high boiling point, which limits their feasibility.[29]

Ultrasonic treatment is not the only form of mechanical energy that can exfoliate graphene sheets. It has been shown, too, that when rotating a tube filled with graphite and *N*-methyl-pyrrolidone at high speed, the mechanical forces are great enough to peel off graphene sheets from graphite.[30] Dispersions of graphene can also be prepared in various liquid polymers. Polymers have usually quite high viscosity and their long structure is ideal for preventing the aggregation of graphene sheets.

A closely related technique to direct exfoliation of graphene in solvents is a surfactant or adsorbate assisted exfoliation. In this technique, graphite is exfoliated, usually via sonication, into solvents that would not dissolve it without the added help of adsorbate molecules. Unlike in the direct exfoliation in solvents, which solvents need to have right Hansen solubility parameters or minimal interfacial energy, in adsorbate assisted exfoliation the adsorbates will stabilize the exfoliated graphene sheets. During sonication of graphite in solvents like water, graphene sheets are constantly exfoliated and dispersed in water but, because of the unfavourable environment, the graphene sheets tend to reaggregate back to graphite. The idea of the added adsorbate molecules is that they will attach to momentarily exfoliated graphene sheets and prevent them to restack. The main requirement for these molecules is that their structure, usually aromatic, will efficiently attach to graphene sheets. Commonly used molecules include anthracene[31] or pyrene[32,33][Paper I] moieties in their structures. These planar aromatic molecules deploy the same π-π –interactions with graphene as graphene sheets have with each other. Also sodium cholate[20,34] and its derivatives [35][Paper I] have been successfully used as adsorbates to stabilize the graphene sheets. Sodium cholate does not have an aromatic backbone like most other common solubilisers. Due to its efficiency of adsorption on aromatic carbon structures sodium cholate based adsorbates have been used to solubilise graphene and carbon nanotubes[36] rather well. In addition to good adsorbate-graphene interaction, the adsorbate molecule should have good solubility in the solvent used and the ability to prevent graphene sheets from restacking. In order for adsorbates to be soluble in water or polar solvents, side chains with highly polar or ionic groups are needed, and amines, sulfonic acids and carboxylic acids are often used. Adsorbate assisted exfoliation is mainly used when graphene sheets are dispersed in aqueous solutions or highly polar solvents but it can be used in other solvents as well. For non-polar solvents long alkyl chains or aromatic moieties are preferred in the adsorbate molecules.

The selection of suitable adsorbate molecules is vast and ever increasing, and choosing the best adsorbate is difficult. The adsorbate molecules have to fulfil certain requirements in order to successfully attach to the surface of graphene and solubilise the sheets. An adsorbate molecule has to replace the solvent layer on top of the graphene surface. Palermo et al. tested series of functionalized pyrenes (1-pyrenesulfonic acid, 6,8-dihydroxy-1,3-pyrenedisulfonic acid, 8-hydroxypyrene-1,3,6-trisulfonic acid and pyrene-1,3,6,8-tetrasulfonic acid), which have an increasing number of sulfonyl groups.[37] They found out that the adsorption of pyrene derivatives on graphite was poorer for derivatives several SO_3^- -groups, making 1-pyrenesulfonic acid the most efficient adsorber. However, pyrene with two SO_3^- -groups was the best solubiliser of graphite. They concluded that high molecule/graphene adsorption free energy and high molecular dipole were the most important factors contributing to the success of 6,8-dihydroxy-1,3-pyrenedisulfonic acid as a solubiliser. The molecule easily slid onto the graphene surface with its hydroxyl groups first, thus allowing the pyrene structure to attach to graphene.

In addition to molecular adsorbates, polymeric adsorbates have been used to solubilise graphene sheets. too. While most molecular adsorbates are ionic and, therefore, an ionic repulsion keeps the sheet from aggregating, polymeric adsorbates are usually non-ionic. They relay mostly on steric hindrance of the long polymer chains.[38] In fact, the highest graphene concentrations with polymeric adsorbates have been achieved by using non-ionic ones. Polymers with linear structure, such as polyvinylpyrrolidone[39,40] or quinquethiophene-terminated poly(ethylene glycol)[41], and branched polymers like poly(ethyleneimine)[42], have been used. Hersam et al. used 19 different Pluronic and Tetronic copolymers in their work.[43] The graphene sheets coated with non-ionic polymers can be easily prepared in various organic solvents or transferred to them. The polymers are also tightly bound to graphene and, in the case of non-ionic polymers, the stability of the dispersion is not affected by pH changes or addition of salt, unlike with ionic polymers or small molecular adsorbates.[44] With many polymer adsorbates, the initially low graphene concentration can be increased by concentrating the dispersion or by completely evaporating the solvent, leaving graphene-polymer –composites. Graphene-polymer –composites are, however, a field of their own, and are not discussed here.

The achieved graphene concentrations using adsorbate assisted exfoliation are often relatively low regardless of the type of the adsorbate,either a small molecule or polymer. The choice of the adsorbate molecule affects the exfoliation and solubilisation but an even more important factor seems to be, e.g., sonication power or time. Generally, the longer the sonication time the higher the graphene concentration.[34] On the other hand, too intense sonication seems to promote aggregation rather than exfoliation, probably because of the detachement of the surface-bound molecules.[35] While sonication is by far the most used method to assist the exfoliation of graphene sheets, other exists other methods to apply mechanical force to graphene, too. Quite recently, direct exfoliation in organic solvents and adsorbate assisted exfoliation could both be scaled to industrial scale, with batch sizes up to 300 litres, by using a powerful mechanical mixer.[20]

Recently, Notley published an improved adsorbate assisted exfoliation method, where adsorbate was constantly added to the mixture during sonication.[44] The idea behind this is that there is an ideal graphene-to-adsorbate ratio for every adsorbate where graphene can be exfoliated the most effectively.[32,35,44,45] As graphene is exfoliated and adsorbate molecules are attached to the graphene surface, the free adsorbate concentration drops and the optimal concentration ratio is lost, causing less effective exfoliation. By keeping the concentration ratio constantly at the optimum level, Notley managed to achieve graphene concentrations as high as 15 mg/ml by using polymeric adsorbates and almost as high concentrations with molecular adsorbates.[44]

Several possible interactions exist between graphene sheets and the adsorbate molecules (molecular or polymeric). The adsorbates often have electron donating or withdrawing groups and tend to dope graphene, the doping level depending on the adsorbate.[46] The adsorbates also affect the hole mobility and minimum conductivity of graphene. An evidence of close contact between adsorbates and the graphene surface is the quenching of adsorbate luminescence, which indicates energy or electron transfer between the two.[47][Paper I] The charged groups in the adsorbate molecules on the graphene sheets allow to use the dispersed graphene as a building block in self assembled structures.

In conclusion, until recently, direct exfoliation of natural graphene in solvents, with or without adsorbates, suffered from low attainable graphene concentration but now seems to have become a considerable option to other manufacturing methods. Some facts has to be taken into account regarding the material produced by direct exfoliation, however. The mechanical and electrical properties of films made of small graphene sheets are inferior to those of a single sheet. In films, small graphene sheets are hold together by weak interactions, rather than by strong covalent bonds within a single graphene sheet. Similarly, the conductivity of a single sheet is higher than conductivity in films, which is limited by charge transfer across the sheet-sheet boundaries. In addition, significant amounts of adsorbate or solvent may be left on the graphene surface when the material is used in applications. The solvent and adsorbate molecules between the graphene sheets generally hamper the mechanical and electrical properties of the material.

The stability of exfoliated graphene sheet dispersions varies from publication to publication. The graphene concentration tends to decrease with time but it is possible to achieve the stability in the time scale of months or even years in certain cases.[22,45][Paper I] The common problem with all the mechanical exfoliation and solubilising techniques is that they produce material, which is a mixture of sheets with various size and thickness. This affects the stability of dispersions as larger particles tend to aggregate more easily. However, materials with uniform or narrow size and thickness distribution are often desired. Therefore, some methods have been developed to fractionate the mixtures. Larger aggregates can be easily removed simply centrifugation at low speed or letting them to sediment down. Finer fractionation may be achieved, e.g., by controlled centrifugation, as the larger sheets tend to sediment with lower centrifugal force than the smaller sheets.[34,48] In density differentiation based ultracentrifugation, graphene dispersion is placed in a gel-filled centrifugation tube, where density gradient is formed under rotation.[49] In this method, density differences between graphene sheets with different number of layers cause them to fractionate. Although the regaining of the different fractions from the gel is laborious, this method is probably the only one capable to fractionate few layer graphene sheets according to the number of layers. Similar separation methods can also be used with other water soluble graphene materials, such as graphene oxide and reduced graphene oxide.

The main advantage of the mechanical exfoliation methods is that that they typically produce chemically unmodified graphene. However, because of the uncontrollable nature of the mechanical exfoliation at the molecular level the produced graphene sheets consist usually of more than one layer of graphene. Typically, few-layer graphene forms a large fraction of the exfoliated soluble graphene sheets although a significant portion consists of single layer sheets. Soluble mechanically exfoliated graphene sheets might be a practical material in various composites where small sized particles with large surface area, mechanical strength and good conductivity are desired. The biggest competition for the methods based on the direct exfoliation of natural graphite probably comes from the use of graphene oxide based materials and their post treatment.

1.4. Graphene Oxide

Until recently, the route utilising GO (graphite oxidation, exfoliation and subsequent reduction) has been far superior to other methods for the preparation of graphene based materials. Possibility of gram-scale synthesis, water solubility of the materials involved, high yield and attainable concentrations, and easy processing have guaranteed its popularity. The main disadvantages of the GO preparation include the slightly hazardous synthesis conditions as well as difficulties and losses in the purification process. Recently, the product quality and yield in liquid-exfoliation and CVD processes have been significantly improved and their cost reduced. However, most of the graphene based materials are still made via the GO route. Graphene oxide itself is an extensively oxidized form of graphene prepared from graphite using various strong oxidants. The first method was introduced already in 1859 by Brodie.[50] The Brodie method has been improved later by Staudenmaier (1898)[51], Hofmann and König (1937)[52] and even further by Hummers and Offeman (1958)[53]. More recently, Tour et al. fine-tuned the Hummers method (2010).[54] The main improvements in these modifications focus on the use of more efficient and safer oxidation procedures and oxidants. The Brodie method consists of several repeated oxidation cycles of graphite powder in a mixture of potassium chromate and fuming nitric acid. The Staudenmaier and Hofmann methods use potassium chlorate and the Hummers and Tour methods potassium permanganate as the main oxidant. Nitric, sulphuric and phosphoric acids or their mixtures are used as a solvent in all of these synthesis methods. Nowadays the modifications of the Hummers' method are the most used ones, but also the other methods mentioned above, and their modifications, are extensively used. All these methods use strong oxidisers and also otherwise harsh conditions to oxidise graphite flakes into graphene oxide. This results in a significant portion of double bonds of graphite being broken during the oxidation and various oxygen containing functional groups decorating the surface and edges of the graphite sheets. Regardless of the oxidation method, the graphene oxide produced contains the same type of functional groups but their relative and absolute abundance may vary significantly from one method to another. Methods based on potassium permanganate result in GO with a higher degree of oxidation than those based on K_2CrO_4 or $KClO_3$ as oxidants.[55-57] The Brodie method produces more C-O moieties than the Hummers method, which, on the other hand, results in a higher relative abundance of the carbonyl based (C=O) moieties.[57] Oxidation with permanganate (the Hummers and Tour methods) also yields higher proportion of C=O groups than the methods based on chlorate oxidation (the Hofmann and Staudenmaier methods).[55,56] The carbon-to-oxygen elemental ratio (C/O) is a measure of the degree of oxidation of GO, and it depends on the method used, too. The Brodie method yields a C/O ratio of approximately 2 while oxidation with chlorate or permanganate result in values above 2 or below and around 2, respectively. These accompanying changes in the chemical structure of GO influence the properties of the material

In addition to the nature of the oxidant, the oxidation level of GO can be decreased, e.g., by limited reaction time[58,59], the amount of oxidant[60], and lower temperature[61]. On the other hand, one way to increase the oxygen content in GO is to use multiple oxidations with one or more oxidising agents. For example, in the original GO synthesis by Brodie, the graphite flakes were oxidised multiple times and after the fifth cycle the C/O ratio stabilised around 1.6. [50] In general, with every oxidant there is a maximum oxidation level for graphite[62,63], and the produced graphene oxide has, therefore, a C/O ratio between 1.5 to 2.5, depending on the reaction conditions. The synthesis conditions play the key role in the formation of GO but also the starting material, especially graphite flake size, affects the efficiency of the oxidation.[64]

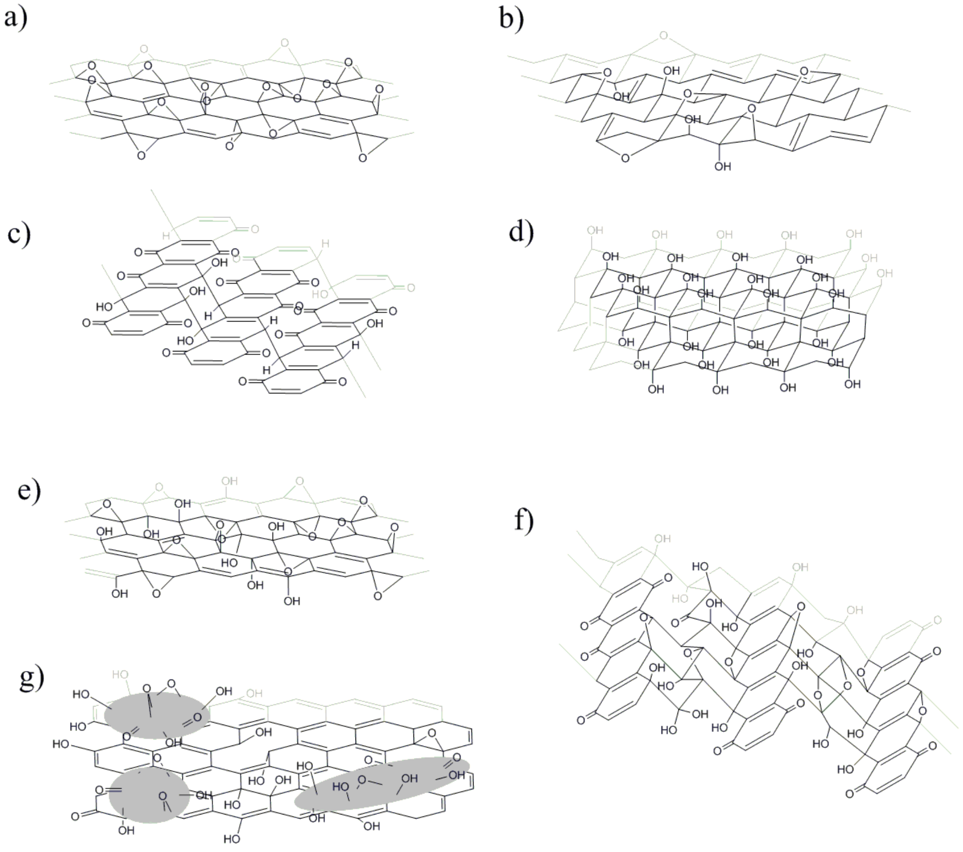

Figure 3. Proposed structural models for the GO.

Even though graphene oxide is composed of carbon, oxygen and hydrogen and synthesised from well-defined graphite material, its the exact structure is not known, even the different types of incorporated functional groups being controversial. The models proposed for GO have been formulated on the basis of theoretical calculations, chemical properties of GO and spectroscopic data. Throughout the years almost all forms of analytical techniques have been used to unveil the exact structure of GO. These methods include elemental analysis techniques, X-ray photoelectron spectroscopy (XPS), vibrational spectroscopy including Raman and IR, UV-Vis and photoluminescence spectroscopy, imaging techniques such as scanning electron microscopy (SEM), transmission electron microscopy (TEM) and AFM, as well as nuclear magnetic resonance (NMR) spectroscopy and X-ray diffraction (XRD). Ambiguous spectral data, limitations in available characterisation techniques and variation in the starting material and synthesis techniques has led scientists to propose several, closely related or sometimes fundamentally different, structures for GO. One of the earliest models for GO was that of by Hofmann and Holst (1939). In this model, the aromatic surface of GO was decorated with only 1,2-ether groups and had a C/O ratio of 2 (Fig. 3a).[65] Later Ruess introduced a structure with *trans*-cyclohexane –based backbone instead of a flat sp^2-based one.[66] Furthermore, Ruess replaced 1,2-ethers with 1,3-ethers and included hydroxyl groups in the structure (Fig. 3b). The Scholz-Boehm – model, a kind of more organised version of the Ruess-model, involves a structure of alternating rows of 1,4-benzoquinones and cyclohexanes with additional OH-groups (Fig. 3c). The Nakajima-Matsuo – model, on the other hand, differs quite significantly from the other models. It consists of a fully sp^3-hybridised structure, where the carbon atoms form two connected atomic layers with only hydroxyl groups decorating the structure, and has a C/O ratio of 2 (Fig 3d).[67,68] A more recent, and also more widely accepted model is the Lerf-Klinowski –model (Fig. 3e).[69-71] It is similar to the Hofmann-model but, in addition to randomly distributed 1,2-epoxides, it includes also hydroxyl groups. Some further versions of this model include additional carboxylic acid groups at the edges of GO sheets, and several other variations have also been made in the light of new discoveries or new interpretations of the old ones. A slightly less popular competing model to the Lerf-Klinowski –model was introduced by Dékány et al.[62] The Dékány-model (also called the Szabó-Dékány –model) is derived from the Scholz-Boehm model and involves quinone/cyclohexane structures with 1,3-ethers and alcohol groups (Fig. 3f). Recently, Tour et al. discarded the idea of a static structure of GO and suggested a more dynamic structure, which can respond to the changes in the external conditions.[72] On the other hand, Rourke et al. proposed recently quite a different idea about the structure of graphene oxide (Fig. 3g).[73-75] They suggested that GO is a bicomponent material composed of relatively unoxidised sheets and highly oxidised small molecules, called oxidation debris, that covers the sheets. This model resembles the mechanically exfoliated graphene, with which the solubility is due to the adsorbates. Their model has lately received increasing amount of interest and cautious support.[76-80]

Although its exact structure remains ambiguous, GO is an extensively used material and its properties have been thoroughly characterize. GO is, due to its charged functional groups, soluble in neutral and basic aqueous solutions but precipitates easily in highly acidic solutions. Electrolytes, even at low concentrations, lead to precipitation, too. The solubility of GO in non-acidic solutions is explained by the acidic nature of GO. In fact, GO has sometimes been called as “a graphitic acid” (Graphitsäure). The zeta potential can be used to estimate the stability of particles in dispersion, and GO has the zeta potential well below -30 mV in aqueous solutions at pH above 4.[81,82] Below pH 4 the zeta potential rises to ca -15 mV, significanly decreasing the stability of aqueous GO suspensions. Kim et al. showed that the level of oxidation of GO affects the zeta potential and they were could change the zeta potential from -30 mV to -50 mV upon increasing the oxidation level.[60] The charged surface groups make GO sheets easily dispersible in water and the electrostatic forces prevent the sheets from aggregating. The various functional groups at the surface of GO sheets increase the possible interlayer distance compared to that in graphite. The GO sheets can interact with each other directly through hydrogen bonding, but because of the hygroscopic nature of GO, some intercalated water is often present between stacked sheets. This intercalated water further increases the interlayer distance of GO sheets from 5.97 Å for a dry sample to 6.91 Å for stacked sheets at 70% relative humidity[62] and, finally, to 12.41 Å for completely hydrated GO stacks[57]. Preparation of water-free GO is difficult due to its high affinity for water and because of the low thermal stability of GO. Another example, which illustrates the special relationship between GO and water, is the impenetrability of GO films to all other gaseous compounds except water vapour and hydrogen gas.[83] The suspendibility of GO is not limited to water but. GO can, in various amounts, be dispersed in some other polar solvents, such as ethanol, 1-propanol and dimethylformamide.[84]

In its physical properties GO differs quite much from pristine graphene. As graphene, GO is also a quite strong material with the Young's modulus of 208 GPa for a single GO sheet[85] but, because of the broken aromatic structure containing functional groups and defects, its mechanical properties cannot compete with pure graphene (Young's modulus 1.0 TPa). However, it is tougher than many polymers and is used, therefore, in polymer composites along with pure graphene and reduced graphene oxide. The presence of functional groups enables GO to bind tighter to polymers than non-functionalised graphene materials. As to its electrical properties, the broken sp^2 –network in GO gives rise to a high electrical resistance in the sheets and makes GO an insulator. Unlike graphite, which withstands temperatures over 1000 °C, GO is quite sensitive to temperature. Upon heating GO powder, already at 50 °C some of the functional groups decompose as carbon dioxide.[86] This kind of thermal decomposition, or graphitisation, is one of the reduction methods for GO, which will be discussed in more detail in next chapter. Graphene oxide is also considered to be behave as a liquid crystal in suspensions containing more than above 0.53 w% of GO[87] and the sheets align themselves under shear stress, forming concentration-dependent fibre or plate-like structures[88].

Graphene oxide is also weakly luminescent. This peculiar excitation wavelength dependant luminescence has raised various theories. It has been attributed either to the functional groups or the aromatic domains of GO, or to the interactions between them.[89,90] Rourke et al., who introduced the oxidation debris –stabilized model of GO, attribute the luminescence of GO to the oxidation debris[75] If GO is treated with strong alkaline solutions, the luminescence disappears and the solubility and colour of GO change, too, while the alkaline washing solution becomes highly fluorescent. This is explained by the removal of fluorescent oxidation debris from the surface of the

GO sheets to the solution by the alkaline treatment.[75] On the other hand, according to their dynamic model of GO, Tour et al. attribute the irreversible changes in the structure of GO in alkaline solutions to the splitting of some of the highly oxidised parts.[72]

In any case, graphene oxide has a range of different functional groups which can be synthetically modified in order to improve the properties of GO. The chemical modification of GO, excluding chemical reduction, will not be covered in this Thesis, but extensive reviews can be found elsewhere.[91,92] The next chapter will discuss the various methods to reduce graphene oxide in order to recover, at least partially, the excellent properties of graphene. Especially, the electrical conductivity is a highly desired property in most graphene-based applications.

1.5. Reduced Graphene Oxide

Reduced graphene oxide does not quite resemble either graphene oxide or graphene but is something in between these materials. It is moderately hydrophobic but can be dispersed in water to some extent, as well as in several organic solvents. It is a rather good electrical conductor but not as good as graphene. Its mechanical properties are closer to GO than pristine graphene. RGO is not as easy to use as GO but it is significantly easier to produce than pristine graphene by reduction from graphene oxide, which can be achieved with a multitude of methods.

The material collectively called *reduced graphene oxide* covers a wide range of different materials which only share the fact that they are made from GO via deoxygenation or reduction, as it is more commonly called. RGO has generally only few oxygen groups left in its structure, making it poorly soluble in polar solvents. The lack of repulsion between the RGO sheets also promotes their aggregation. During the reduction the aromatic structure is partially restored and RGO recovers electrical conductivity. Countless factors at every step of the preparation process affect the properties of the formed RGO. First, the quality, size and source of graphite and, second, the oxidation process used, determine the properties of GO and, therefore, also affect RGO formed from it. GO can be chemically reduced using numerous different reductants or by many nonchemical methods including intense UV radiation and laser or plasma treatment. Even with a single method, e.g., a chemical reduction with hydrazine, the reduction temperature (from room temperature to boiling water), time (from seconds or minutes to hours) and reductant concentration (from millimolar to pure hydrazine) can be changed to adjust the formed product. The differences in RGO, which usually are quite small, might, however, be insignificant or have a profound effect, depending on the intended use of RGO. For example, the impurities left after the reduction may consist of just a few nitrogen atom substituents or a significant heavy metal contamination, or the reduction may remove only certain specific functional groups. The strategy used for the reduction has to be chosen with the application, desired functionalization or the level of reduction in mind. Edwards and Coleman have reviewed the pros and cons of various graphene synthesis routes and discussed their compatibility to various applications.[93] In this chapter some of the most common reduction methods, along with other methods important to this Thesis, will be discussed and their special features explained.

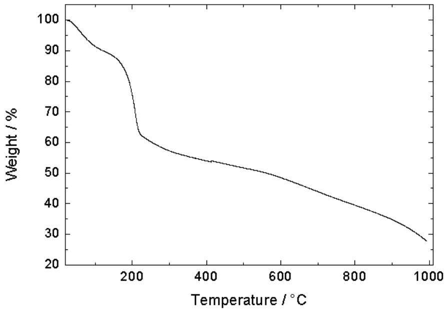

Figure 4. TGA of GO in nitrogen at the heating rate of 5 °C/min.

The most simple reduction method for GO is thermal annealing because dry GO is not thermally stable at temperatures above 150-200 °C. Upon heating, preferably in inert atmosphere, GO undergoes graphitisation. Thermogravimetric analysis of GO show a significant mass loss above 100 °C that corresponds to intercalated water and the most significant removal of oxygen containing functional groups begins at approximately the same temperature (Fig. 4). At approx. 220 °C, most of the functional groups have already been removed from GO. It has been shown, that after 23.5 h of annealing at the 220 °C, the C/O ratio of GO increased from 2.0 to 10.1 and sheet resistance dropped to 8200 ohms per square.[94] The deoxygenation continues slowly up to 1000 °C. At this point, graphene oxide has lost almost all its functional groups. It is not completely understood, what happens during thermal treatment of GO, since there are several possible reaction routes depending on the annealing process and amount of intercalated water in GO. It has been shown that, already at ca 50 °C, some of the functional groups of GO start to break down releasing CO_2, but at higher temperatures CO is formed.[86] In the reaction occurring below 200 °C, the intercalated water molecules are actively involved in the formation of CO_2 [86,95] In these studies water-free GO samples produced only a fraction of the CO_2 compared to water containing samples. According to Acik et al. water forms hydroxyl radicals which further react with the functional groups of GO, producing the CO_2.[95] At higher temperatures, at which most of water has been consumed or evaporated, radical reactions involving other species such as O_2, CO_2 and CO take place. Regardless of the exact reaction mechanism, eventually almost all of the functional groups of GO have been “burned” away as CO_2 or CO. This leaves behind RGO with a minimal amount of oxygen but a moderate amount of holes or defects in place of the functional groups. Annealing in argon at 1000 °C has resulted in RGO with a

C/O ratio of 11.36, and a value of 14.1 has been obtained for GO annealed in ultra-high vacuum at 900 °C.[96] Values as high as these are rarely achieved using chemical reduction. Although the thermal treatment of GO is a simple and effective method, it has some limitations. The obvious drawback in annealing is the fact that GO must be placed on a substrate, which can withstand the annealing temperatures without breaking itself or RGO, or without reacting with GO. Therefore, this method is the best suited for GO films or single sheets on a substrate but may, to some extent, be used for GO dispersed in stable organic solvents.[97,98]

Chemical reduction is by far the most used technique for the reduction of GO. It is done usually in aqueous solutions and can be applied to GO solutions, GO deposited on a substrate or even to GO composites. There is a wide variety of different reducing agent to choose from and the most efficient ones can reduce GO at room temperature or slightly elevated temperatures. Some of the reducing agents are toxic or otherwise dangerous while others are environmental friendly, some of them chemically modify RGO, while others reduce GO purely. Chua and Pumera recently focused on the properties of a variety of reductants in their review, covering altogether fifty different reducing agents.[99] These include, e.g., borohydrides, aluminium hydride, hydrohalic acids, metals, and, some biomolecules and plant extracts, too. The emphasis was on known and proposed reduction mechanisms of different reducing agents and their reduction efficiency. Despite good understanding of the chemical reactions involved with some of the reducing agents, many of the processes in the GO reduction are not known. In fact, the uncertainty about the structure of GO does not help the understanding of the chemistry of GO, either.

The most common reducing agent is hydrazine, despite of its explosive and toxic nature. It has become a kind of reference for other reducing agents and methods. Hydrazine was one of the first reductants employed in graphene oxide reduction and still is considered a rather good one. It is highly reactive and reacts with GO already at low temperatures or at low concentrations, effectively removing most of the oxygen containing functional groups. Although hydrazine is usually used as a dilute aqueous solution, it has also been used as a “solvent” for GO during reduction. Hydrazine-based reduction involves several known reaction mechanisms, which can remove oxygen functionalities and restore C=C bonds.[99] Ideally, hydrazine acts as a four electron donor, and breaks down to nitrogen gas and water upon reaction with oxygen functionalities, but normally it is a two electron donor producing N_2H_2. Although this is the main reaction route, a significant portion of nitrogen is left in the RGO structure after the reduction. In our own work on hydrazine, we found that the C/N atomic ratio was 5.9, indicating a heavy nitrogen doping in hydrazine-reduced GO. [Paper II] It has been shown that hydrazine produces a nitrogen containing ring structure, pyrazole, at the edges of RGO.[100] This type of substitution acts as a dopant for RGO and affects its the electrical properties. The mechanical strength of a GO paper, made by filtering a GO suspension, is rather similar before and after reduction with hydrazine, followed by thermal annealing. A GO paper reduced with hydrazine has a Young's modulus of 20.5 GPa, which increases to 41.8 GPa, if the paper is further thermally annealed at 220 °C.[101] On the other hand, a Young's modulus of 25.6 GPa has been reported for a GO paper, a value in the same range than that for a reduced GO paper.[102]

Various metals constitute another group of chemical reducing agents. Several elemental metals and metal ions are capable of reducing GO. For example, Al, Zn, Fe, Ti(III) and Sn(II) have been successfully used for this purpose. Upon reduction of GO, some of these metals tend to form oxides with the oxygen removed from GO. These oxides are sometimes soluble and are removed from RGO but, with certain metals, remain on the surface of RGO. Positive metal ions can also form complexes with negative groups in GO and RGO. Metals or metal oxides left on the RGO sheets may add some properties to the material, such as magnetism or light sensitivity in case of iron oxides or TiO_2, respectively.[103,104]. Depending on the metal, the reduction reaction can take place in acidic (Al, Fe, Zn, Sn(II), Ti(III) and Mg) or basic (Zn, Al and Na) solutions.[99,104]

A common reducing agent in organic chemistry, sodium borohydride, has also been used to reduce GO. $NaBH_4$ efficiently reduces certain carbonyl groups to hydroxyl groups, providing a way to selectively reduce only some of the functional groups in GO, and leading to a partially reduced GO, which can be further reduced with other reductants or functionalised with suitable groups. This strategy has been used, especially, for adding groups to promote solubility in selected solvent as reaggregation is a constant problem with RGO. Samulski et al. used first $NaBH_4$ to convert C=O to C-OH and then substituted the hydroxyl groups with *para*-phenyl sulphonic acid groups before final reduction with hydrazine.[105] Other partial or selective reduction methods have also been developed. Lithium aluminium hydride ($LiAlH_4$) is a slightly more efficient reducing agent than $NaBH_4$ and can convert also COOH groups to OH groups.[106] Chua and Pumera[107] built on this idea and used ethanethiol-aluminium chloride complexes to remove OH-groups from GO.

1.6. Electrochemically Reduced GO

As mentioned, some metal/metal ion –pairs have high enough reducing power to reduce GO. In electrochemical reduction of GO, similar reduction potentials are created using external voltage. Electrochemical reduction has gathered significantly less attention than chemical methods despite its several advantages. Electrochemistry offers an alternative method that can be extremely simple and environmentally friendly. Simply by depositing graphene oxide on top of a working electrode and placing the electrode, together with a counter electrode, in any aqueous electrolyte system and applying a -1 V potential between the electrodes, GO can be turned to RGO. For the research purposes 3-electrode systems are preferred.

Electrochemical reduction of GO is generally done in aqueous solutions, in which the reduction potentials vary between -0.6 V and -1.1 V (vs. Ag/AgCl) depending on the pH, well within the potential window of water in these conditions.[108][Paper IV] Various working electrode materials can be used, including gold, glassy carbon and conductive glasses. In electrochemical reduction, various oxygen-containing groups are reduced. However, the resulting physical changes of the material may cause delamination from the electrode and hamper its further use.

Electrochemical reduction is not limited only to aqueous solutions but can be carried out in various organic solvents, too.[Paper IV, Paper V] In organic solvents, the used reductions potentials are generally more cathodic leading to more complete reduction of GO. In some cases, such as in solar cell and transistor applications, water may be detrimental and the use of organic solvents is highly beneficial.

Electrochemical reduction requires GO to be deposited on a conducting substrate, which can be seen as a limitation of the electrochemical method compared to chemical methods. However, covering a conducting substrate with another conducting material, e.g., graphene, has a crucial role in some devices. For example, applications in photovoltaics or sensing require a conducting surface with special properties, such as a suitable work function or large surface area (2630 m^2g^{-1} for graphene).[109] On the other hand, several factors may prevent an efficient electrochemical reduction of GO in solutions. First, GO generally has a negative charge in aqueous media, which may expel the GO sheets away from the electrode surface at highly cathodic potentials required for reduction, although this is mainly problem in extremely dilute solutions. Second, the formed RGO is hydrophobic and, therefore, will not be soluble in aqueous media but precipitates on the electrode. The use of certain adsorbates and high speed stirring may prevent the accumulation of RGO on electrode surfaces and help solubilise the material. Third, GO suspensions are highly sensitive to ionic strength and tend to precipitate already at very low salt concentrations. A solution may be to use GO itself as a supporting electrolyte in the electrochemical cell because it is charged at all pH above 2 and can be considered a kind of polyanion.[110]

Electrochemical reduction can be applied to films of GO of any size or shape, as long as they are placed on a conductive surface. A thin GO layer on an electrode surface will be rapidly reduced, which can be seen in the cyclic voltammogram of a monolayer and thin film of GO, as the current related to reduction is seen only during the first cathodic scan. With thicker films, the reduction progress is slower. [Paper IV] Dong et al. have reported an electrochemical reduction technique, which does not require the GO film to be placed on a conductive surface. In their method, an external (small diameter) working electrode is pressed on the GO film during reduction, which also allows the patterning of the GO film with reduced domains.[108]

In conclusion, the electrochemical reduction of GO allows good control over the reduction process and is, therefore, a valuable method for research purposes as will be shown later.[Paper III, IV and V] Another benefit of the electrochemical reduction of graphene oxide is that it also enables an easy preparation of composite electrodes for various applications. For example, GO can be mixed up with various electropolymerisable monomers, such as pyrrole, EDOT etc., and GO can be reduced during or after the electrochemical polymerisation of these monomers, which form a polymer matrix that entraps the GO.[110,111] Composites could also be prepared by depositing GO with other materials, such as conductive polymers, on the electrode by spin coating, ink jet printing or some other means, and performing the electrochemical reduction afterwards.

2. Aims of the Thesis

The work in this Thesis has its origin in the desire to begin research on graphene in our laboratory. Intense work has enabled us to develop novel manufacturing routes to graphene materials and to apply sophisticated characterisation methods on these materials. Producing graphene material is challenging, especially in large scale and at high quality. Due to the lack of an universally applicable preparation technique, a wide range of satisfactory methods exist. Therefore, the competition to find ever better techniques is raging. While many of the fundamental properties of graphene have been discovered, there are still much new discoveries to be made in the properties of graphene based materials as well as in their applications.

The focus of Paper I was to find a suitable chemically non-invasive method for producing aqueous graphene sheets. With the help of ultrasound induced mechanical forces and suitable adsorbate molecules, this was achieved. This opened up an opportunity to investigate the nature of the interactions between various adsorbates and the graphene.

Papers II, III, IV and V are focused on graphene oxide and its various reduction methods, which can efficiently convert this highly damaged material back to graphene. In Paper II, surprising discoveries were made using vanadium as a chemical reducing agent for GO reduction.

Chemical reduction methods are replaced with electrochemical methods in Papers III, IV and V. *In situ* spectroelectrochemistry makes possible to control and monitor the reduction process of GO in great details.

The overall aim for this work is to open up new possibilities to produce graphene based materials and to better understand their properties and related phenomena.

3. Experimental and Characterisation Techniques

3.1. An Introduction to Common Characterization Methods for Graphene Materials

Pristine graphene is in many ways an uninteresting material to characterize because it consists only of identical aromatic carbons. This means, that with most spectroscopic techniques, only a few bands are seen. Perhaps the most important spectral characterization method for graphene is Raman spectroscopy. It can be used, e.g., to estimate the thickness of the graphene sheets as well as the ratio of edges and other defect sites to pristine graphene sites but also more subtle details such as of doping of graphene sheets. The use of Raman spectroscopy for graphene and graphite research has been discussed in detail in many publications[112,113] and, therefore, only the most central features are discussed here. In pristine graphene, there are only two very sharp spectral features: the G and G' bands. The excitation wavelength independent G band originates from the pristine aromatic structure of graphene and appears at ca.1600 cm^{-1}. It is sensitive to changes in graphene structure and can be used to monitor them. The G' band (also called the 2D band), unlike the G band, is dependent on excitation wavelength and appears approximately at 2700 cm^{-1}. By analysing the shape of the G' peak, information about the thickness of graphene particles can be obtained because single and few layer graphene sheets both have unique peak shapes.[114] Structural defects in graphene structure, including sheet edges, give rise to another Raman active vibration called the D band. The D band corresponds to breathing modes of the carbon rings located next to the defect sites. This band can become intense in very small graphene fragments and, especially, in highly oxidized GO particles. The D band position depends on the excitation wavelength, too, and decreases linearly from 1360 cm^{-1} (with excitation at λ_{ex} = 488 nm) to 1325 cm^{-1} (excitation at λ_{ex} = 647.1 nm) [115]. The position of the D band at 1300 cm^{-1} using near-infrared excitation at 1064 nm (the Raman instrument mostly used in this work) is well in accordance with this behaviour.[Paper I]. The Raman spectra of graphene based materials exhibit also several weaker bands, often seen only as small shoulders close to stronger bands. The analysis of the Raman spectra is complicated, which may give rise to contradicting interpretations.[116] For example, both the increase and decrease of the D/G intensity ratio, as well as red and blue shifts of the bands have been reported upon reduction of GO. Many phenomena, for example doping[117] and temperature[118] affect the intensities, positions or widths of the bands.

Two common X-ray techniques, the X-ray photoelectron spectroscopy and X-ray diffraction, are often used in graphene research. The XRD is less useful with plain graphene but gives more information about thicker structures and the packing of graphene and modified graphene. The XPS is applied to acquire information about the elemental composition of materials and the chemical environment of the atoms. With graphene, only aromatic carbons should be observed, except for some minor sp^3 carbons at the edges. The XPS offers much information about chemically modified graphene, such as GO, because it can be used to calculate the C/O ratio and to identify the type of oxygen functionalities.

Infrared spectroscopy (IR) is rather useless for pure graphene since it has practically no IR active vibrations. Only a weak band due to a C=C bond related vibration might be detected. The IR spectrum of GO, on the other hand, is a completely different story. It is filled with different oxygen related vibration bands, which are difficult to identify due to overlapping of broad bands and the multiple closely related vibrations. This huge difference between the spectra of GO and graphene makes IR quite a useful tool for monitoring the oxidation of graphene or the reduction of graphene oxide.

For functionalised graphene, nuclear magnetic resonance spectroscopy has been used to identify the structures involved, too. Due to poor solubility of most graphene materials, the use of a solid state NMR is often required. Furthermore, labelling of hydrogens with deuterium in the functional groups of GO, or ^{13}C-enriched graphene can be used[119]. IR, XPS and NMR are often used together to solve structural problems connected to GO or other modified graphene materials. Despite of these powerful techniques an agreement about the structure of GO is still missing.

A single layer of graphene is more than 97% transparent in the visible range and shows only a single absorption band in the UV-vis absorption spectroscopy. In graphene, this band at ca. 270 nm corresponds the π-π^* transition. In GO, this band shifts to 230 nm and another peak emerges, a n-π^* transition at 300 nm. Usually, the UV-Vis –absorption spectrum is used to measure the concentration of graphene based solutions utilising the dispersive tail at higher wavelengths. Graphene oxide is also weakly luminescent, when pristine graphene shows no sign of luminescence.

Various imaging techniques are often used to measure the number of graphene layers in structures and to study the arrangement of the graphene based particles in films or composites. These techniques include atomic force microscopy, scanning electron microscopy and transmission electron microscopy. AFM is good for identifying separate sheets on smooth surfaces and for the estimation of sheet size and thickness. It gives information about small areas only but can be used in various types of measurement set-ups including conductivity and nanoindentation on a single graphene sheet. With SEM, larger areas or structures can be studied. Some SEM instruments may also use an energy-dispersive X-ray spectroscopy technique (EDX) to record elemental spectrum of the investigated material. The EDX is less sensitive than XPS and shows only the amount of elements but gives no information about their chemical environment. TEM requires thin samples but the measurements suffer somewhat from the transparency of graphene sheets. In the selected area diffraction (SAED) mode TEM can map the atoms in graphene materials and reveal the number of graphene layers or defects within the sheets.

3.1.1. Specialised Characterisation Techniques Used in This Work

Many of the characterisation methods mentioned in previous chapter were used also in this work and in the publications included (Papers I-V). Papers III, IV and V focus on the electrochemical reduction of GO and, especially, the *in situ* spectroelectrochemical methods in Paper III and Paper V required some specialised setups for spectral recording. Generally, spectroelectrochemical methods allow a precise control of the state of the material through applied potential while, simultaneously, the spectrum of the material can be measured. However, the experimental configurations of the measurement systems in spectroelectrochemistry may be complicated, and can have a deteriorating influence on the spectral and electrochemical signals. Furthermore, a spectral interference caused by electrolytes is possible. In Paper III, surface enhanced infrared spectroscopy (SEIRAS) and surface enhanced Raman spectroscopy (SERS) are used in the *in situ* mode. In Paper V, both traditional Raman spectroscopy and SERS were used together with *in situ* IR spectroscopy but the latter without the surface enhancement. For the IR methods, with and without surface enhancement, a Kretschmann –type attenuated total reflection (ATR) configuration was used. The basic experimental arrangements used in these measurements are presented in Fig. 5 and described in more detail below.

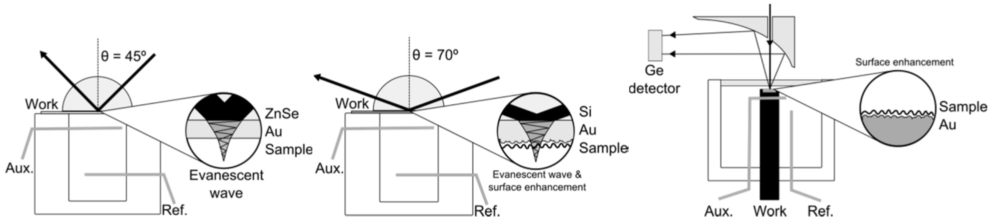

Figure 5. *In situ* setups of (left) single reflection ATR, (middle) SEIRAS and (right) SERS measurements used in this work. SEIRAS and ATR utilise Kretschmann type geometry. All the cells have golden working electrodes, Pt-wire for auxiliary electrode and Ag/AgCl pseudo-reference electrode for electrochemistry.

The modified Kretschmann type setup consists of an internal reflection element (a silicon half cylinder in Paper III and a ZnSe hemisphere in Paper V), which is covered with a thin layer of metal, such as gold. Due to the shape of the reflection element, the angle of the incoming radiation can be varied. The Kretschmann geometry is normally used in the surface plasmon resonance technique, in which the alignment of the IR beam is highly important in order to generate the plasmon resonance. However, this work did not make use of the surface plasmon resonance and the Kretschmann geometry was used in single reflection ATR type measurements only. In attenuated total reflection infrared spectroscopy, the IR beam enters the internal reflection element with an angle of incidence higher than the critical angle, resulting in the total reflection of the IR beam. If a material with a suitable refractive index is placed on the surface, where the total reflection occurs, an evanescent wave is created in the coating material. This coating can itself be a sample material or, like in our case, a thin gold layer covered with a sample. Because the evanescent wave does not extend deep into the layer covering the reflection element, the underlying gold layer between sample and the element must be very thin.

If the surface enhancement effect is wanted in the IR or Raman measurements, special attention must be paid to the electrode surface. The surface enhancement is achieved in SERS and SEIRAS by using a rough gold surface, which is formed electrochemically and by chemical deposition of gold nanoparticles, respectively. Suitable surface roughness, i.e. particle size, is determined by the excitation wavelength and material used. The surface enhancement effect is especially strong in SERS but is also significant enough in SEIRAS to enable both techniques to study monomolecular layers on the electrode surface.

In situ surface enhanced Raman spectroscopy was performed using electrochemically roughened gold electrodes and an in-house built electrochemical cell. The electrochemical roughening process of the gold electrode has been reported elsewhere.[120] The sample deposited on the gold electrode is excited through a glass window using a 1064 nm Nd:YAG Raman laser and the backscattered signal is recorded by a germanium detector (Fig. 5). In dispersive Raman measurements, a laser with 514 nm excitation was used instead.

3.2. Analysis of Our Graphene Materials

In this work, we prepared graphene materials using various techniques. Paper I focuses on mechanical exfoliation of graphene from natural graphite. Other papers, Paper II, III, IV and V, are dealing with reduction of graphene oxide. In the chronologically first publication, Paper III, we used GO which was produced in Nanyang Technological University, Singapore. They used SP-1 natural graphite (Bay Carbon) and oxidised it using a modified Hummers method, which included a pre-oxidation step. For the other publications dealing with GO, Paper II, IV and V, we prepared GO in our laboratory. We used natural graphite from Alfa Aesar (mesh 325) and another version of the modified Hummers method. In Paper I, the same natural graphite powder was used as in Papers II, IV and V.

The synthesis of the Singaporean GO was adopted from a publication of Kovtyukhova et al. [121] and used in a slightly modified way [122]. In their GO synthesis, graphite powder was pre-oxidised in sulphuric acid with $K_2S_2O_8$ and P_2O_5. The pre-oxidised GO was then oxidised with a modified version of the Hummers method, in which $NaNO_3$ was not used. In this secondary synthesis, only $KMnO_4$ in sulphuric acid was used as an oxidant. Unfortunately, we had only limited characterisation data about this material and we could not comprehensively compare it to our own GO. Based on the data and knowledge we have, the differences are not substantial, and most likely, consist of slight differences in oxidation level. The main oxidant, $KMnO_4$, was used for both GO synthesis and most likely produces rather similar functional group distributions in both cases.

For our own GO synthesis, we used a down-scaled version of the modified Hummers method suggested by Hirata et al. [58]. This version of the Hummers method uses the same mutual ratios of H_2SO_4, $KMnO_4$ and $NaNO_3$ than the original Hummers method[53] but twice the amount of graphite and considerably longer reaction time. The reactants and their amounts in the original and modified Hummers method are listed in Table 1. In the modified synthesis route, graphite, sodium nitrate and concentrated sulphuric acid are mixed together in an ice bath. The mixture is then stirred in the ice bath and potassium permanganate is slowly added to it. The mixture is then slowly let to warm up to room temperature and kept stirred for five days. Then diluted sulphuric acid is added to the mixture. Finally, excess permanganate is consumed by addition of hydrogen peroxide and the GO mixture is centrifuged. We developed a purification method where the precipitate is purified by repeated dispersion in distilled water and centrifugation. After the pH of the GO mixture is slightly raised the purification is finished with extensive dialysis. The GO is dialysed against distilled water in a cellulose dialysis tube with a molecular weight cut off of 3500 Da.

Table 1. The amounts of reagents in original Hummers method[53] and modified Hummers method used in this Thesis work. The modified Hummers method is a down-scaled version of a method by Hirata et al. [58]

Method	**m(Graphite)**	**V(conc. H_2SO_4)**	**m($KMnO_4$)**	**m($NaNO_3$)**
Hummers	100 g	2.3 l	300 g	50 g
Modified Hummers	2 g	68 ml	9 g	1.5 g

In order to give as accurate information as possible about our experiments with GO, the GO used in Papers II, IV and V will be analysed next. This is because the properties of the starting GO material have a huge effect on the produced RGO.

According to the XRD measurements on the pristine natural graphite (Alfa Aesar, mesh 325), there is a single 2θ peak at 26.55 degree corresponding to a basal plane reflection of graphite, which indicates an interlayer distance of 0.344 nm. This is close to the expected value of 0.335 nm. For graphene oxide the basal reflection is shifted to 11.4 degree, indicating an interlayer spacing of 0.779 nm between the GO sheets.

By using another other X-ray technique, XPS, graphene used in this work was shown to consist of carbon and oxygen only, with only negligible sulphur impurities (Fig. 6). The most significant features in the survey spectrum correspond to signals from oxygen 1s, at ca 533 eV, and carbon 1s at ca 285 eV. Deconvolution of the spectra could not be reliably done in case of oxygen due to multiple overlapping bands, but for carbon the signals attributed to C=C/C-C (284.8 eV), C-O (286.9 eV), C=O (288.0 eV), and O-C=O (289.0 eV) bonds could be identified. The π-π^* satellite might also slightly contribute to the peak at 289.0 eV. Figure 6c shows that, in the C 1s spectrum of GO, the oxygen connected carbons dominate. The approximate fractions of the various carbon types are 44.5 %, 45.4 %, 7.7 % , and 2.4 % for the C=C or C-C bonded, C-O bonded, C=O bonded and O-C=O bonded carbon atoms, respectively. The total C/O ratio of our GO was 2.3, which is well in accordance with typical GO, although representing a slightly lower oxidation level than typically in permanganate oxidised graphene oxide.

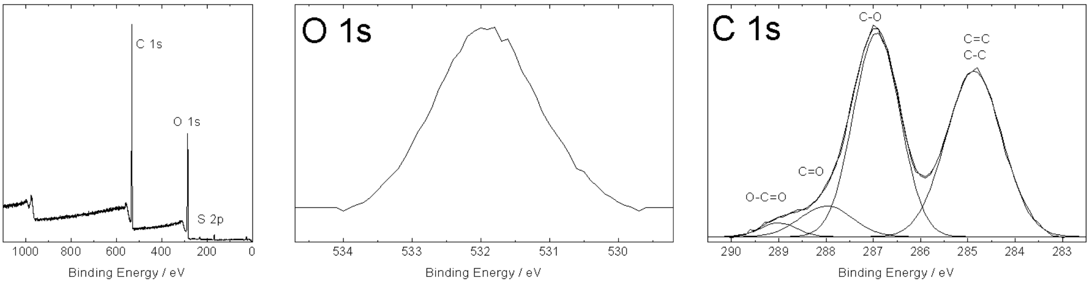

Figure 6. XPS results of GO with survey spectrum of whole range (left), oxygen 1s (middle) and carbon 1s spectrum with fitted C=C, C=O, O-C=O and C-O (right). [Paper II]

The functional groups of graphene oxide can also be seen with IR spectroscopy (Fig. 7). Various carbonyl groups show a stretching vibration peak at 1740 cm^{-1}, accompanied by a shoulder at 1820 cm^{-1}. Intact C=C bonds have a weak stretching vibration at approx. 1570 cm^{-1}, which is strongly overlapped by the bending vibrations of adsorbed water molecules at 1620 cm^{-1}. When GO is reduced it becomes hydrophobic and the C=C structure partially restored, which makes the C=C vibration dominant in this region. The range of spectrum between 1500 and 1000 cm^{-1} contains several different C-O vibrations. The first (1380 cm^{-1}) of the three main peaks originates from bending vibrations of hydroxyl groups or carbonates of GO.[62] The second peak at 1240 cm^{-1} could be due to either epoxides[123] or phenols[62]. The last of the three peaks belongs to C-O vibrations but also to C-C stretching vibrations of the possible sp^3 carbons. The huge broad vibration band above 3000 cm^{-1}

consists of O-H vibrations (peaks around 3300 and 3600 cm^{-1}) of the hydroxyl groups, as well as those of intercalated and free water molecules (producing very broad bands). Sometimes a more detailed interpretation of the vibration bands of GO is performed in order to fit the results better to some of the structural models of GO.

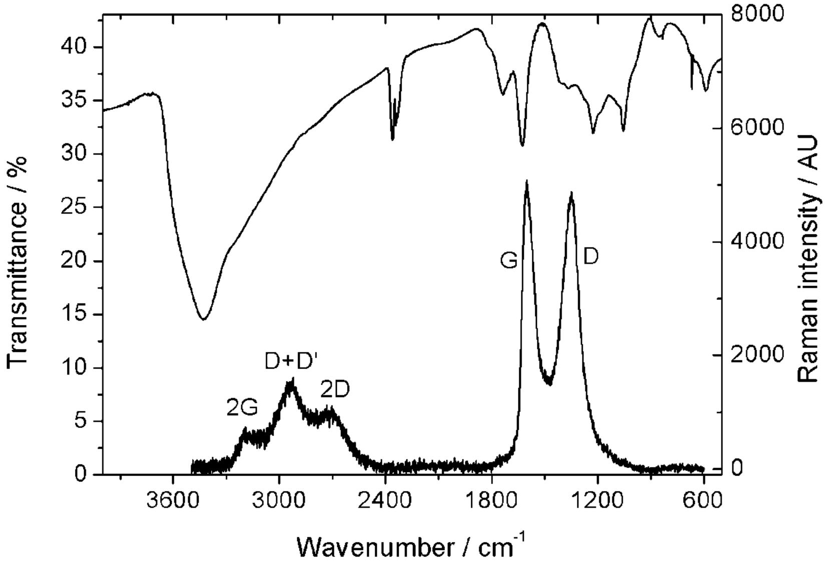

Figure 7. IR (above) and Raman (below) spectra of GO. IR spectrum was measured from freeze-dried GO in KBr pellet and Raman spectrum from thin GO film deposited on gold using 514 nm Raman laser.

Our graphene oxide exhibits the traditional D band at 1350 cm^{-1} and the G band at 1605 cm^{-1} in its Raman spectrum (Fig. 7). The G band hides also a weak D' band which, like the D band, originates from defect sites. A broad band between 2400 and 3300 cm^{-1} can also be seen in the spectrum, with tree individual peaks assigned to the 2D (G') at 3200 cm^{-1}, D+D' at 2930 cm^{-1} and 2G at 3200 cm^{-1} modes. These represent sum or multiple modes of the original G, D and D' bands. The UV-Vis spectral analysis of GO showed only a single band at 230 nm, corresponding to a π-π* transition, and a shoulder from n-π* transition at 300 nm, as expected.

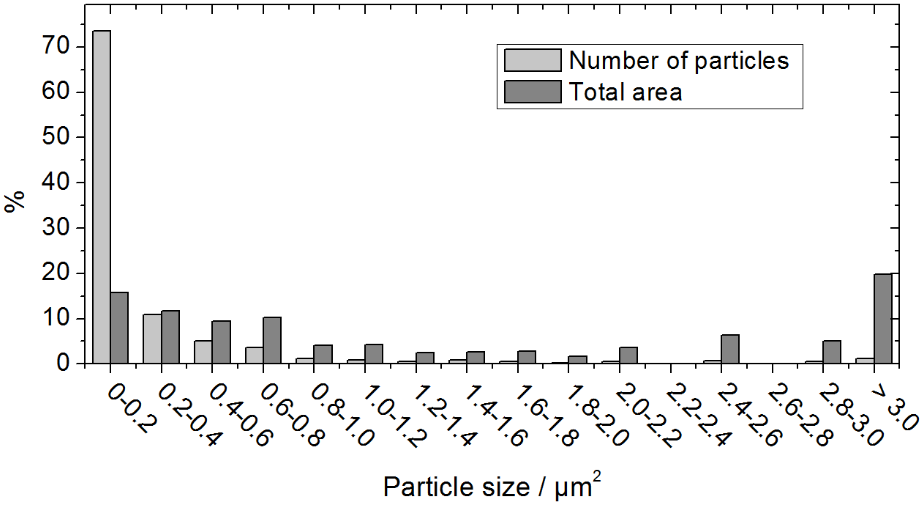

Figure 8. Diagrams based on AFM measurements show the size distribution of GO particles based on total area and number of particles.

The GO used in most of our work consists of mainly small GO sheets. Over 94 % of the GO particles are less than 1 µm^2 in size and only few sheets larger than 3 µm^2 exist. However, the small sheets (< 1 µm^2) represent only approximately 60 % of the total surface area of the material. In the AFM images, individual sheets can be clearly distinguished and some overlapping or folding of the sheets seen. The thickness of the sheets on a silicon substrate is close to 1 nm, which is typical for a value of a single sheet in AFM measurements.

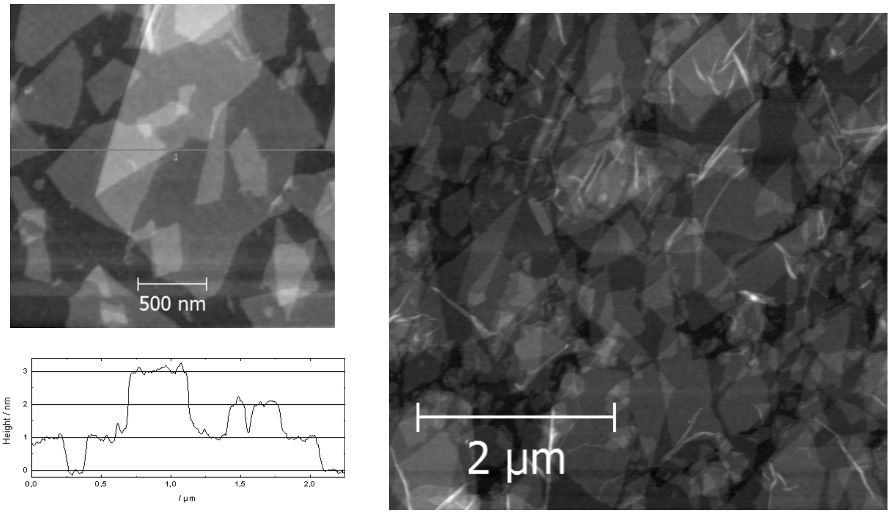

Figure 9. AFM image of GO shows clearly the single GO sheets and in the profile view 1 nm steps can be observed when moving from substrate to single, bi- or tri-layer GO sheets.

To conclude, we have used natural graphite for the direct exfoliation to graphene and for the preparation of graphene oxide. The GO produced in our laboratory consists of mainly GO sheets with a lateral size less than one micrometre and the C/O ratio of 2.3. Significant impurities could not be found in GO.

4. Results and Discussion

In the following chapters, natural graphite is used in various ways to produce graphene and graphene based materials.

4.1. Mechanically Exfoliated Graphene

Mechanically exfoliated single layer graphene and few layer graphene sheets are usually prepared by sonicating graphite and adsorbate molecules in water. We originally adopted our technique from the solubilisation of carbon nanotubes with same technique and under similar conditions.[36] In this technique, we used additional mechanical mixing of the two compounds before sonication. To do this, graphite powder and the adsobate were grounded with mortar and pestle about 10 to 15 min. After sonication in water for one hour with a tip sonicator, the unsoluble precipitate was separated and the produced exfoliated water-dispersed graphene was purified from excess adsorbate using dialysis. As the adsorbates we selected a variety of different ionic organic molecules and a few ionic polymers (Fig. 10) that all have previously been used to solubilise other carbon materials. In addition to the molecules shown in figure 10, also Gum Arabic (GA), a natural mixture of saccharides and glycoproteins, was used.

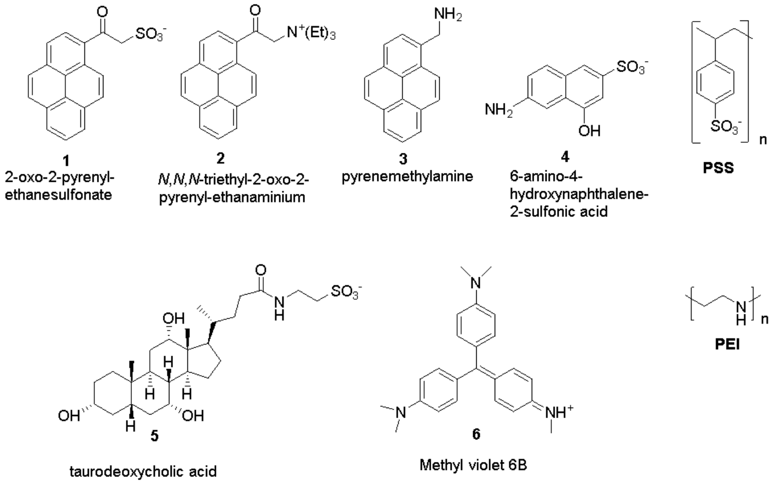

Figure 10. Molecular structures of adsorbates used to solubilise graphene sheets. Molecular adsorbants were numbered from **1** to **6** and abbreviations PSS and PEI were used for polystyrenesulfonate and polyethyleneimine, respectively.

The formed adsorbate/graphene composites, marked as **G-1**, **G-2** and so on, were then characterized. Concentrations of graphene or few layer graphene were calculated from UV-Vis spectra using absorptivity values of $\alpha(660\ \text{nm}) = 24.60\ \text{ml mg}^{-1}\ \text{cm}^{-1}$ and $\alpha(900\ \text{nm}) = 28.0\ \text{ml mg}^{-1}\ \text{cm}^{-1}$, the former based on the literature[33] and the latter on our estimation using reduced graphene oxide. The concentration values were not especially high, varying between 0.006 and 0.048 mg/ml but are typical for this kind of technique, as discussed in chapter 1.3. Although there was not a clear correlation between the particle zeta potential and the composite concentration, anionic solubilisers performed generally better than the cationic ones. Higher concentrations should be possible to achieve with the selected adsorbates by careful optimisation of concentrations, sonication time and power[34,35], or using other improved exfoliation techniques discussed earlier. While the produced composite material does not generally contain much single layer graphene, there is often a significant fraction of few layer graphene present (Table 2). Especially, molecule **5**, taurodeoxycholic acid, produced mainly few layer graphene and a large fraction of single layer graphene. Polymeric adsorbates, on the other hand, form generally larger and more spherical structures than the molecular ones.

Table 2. Graphene concentrations, zeta potentials and sheet thickness fractions of graphene based composites.

Composite	Concentration (mg/ml)		Zeta potential (mV)	Fraction of sheet thickness (%) [c]	
	660 nm [a]	900 nm [b]		< 2 nm	< 5 nm
G-1	0.024	0.019	-35	10	36
G-2	0.012	0.009	+20	n/a	n/a
G-3	0.008	0.006	+25	33	70
G-4	0.020	0.015	-34	7	17
G-5	0.023	0.018	-42	65	90
G-6	~0.012	0.008	-13	2	9
G-GA	0.026	0.022	-27	n/a	n/a
G-PEI	0.021	0.017	+58	14	46
G-PSS	0.057	0.048	-53	n/a	n/a

[a] Based on α(660 nm) = 24.60 ml mg^{-1} cm^{-1}

[b] Estimated based on α(900 nm) = 28.0 ml mg^{-1} cm^{-1} for RGO

[c] Areal fractions based on AFM measurements.

The UV-Vis spectra also revealed that, in many cases, the absorbance bands of the adsorbates on the graphene surface were slightly red or blue shifted when compared to free molecules. The bands of adsorbed aromatic molecules were generally broadened, too. [Paper I] These changes indicate interactions between graphene sheets and the adsorbate molecules and changes in the interactions between the adsorbate molecules themselves. The graphene-adsorbate interactions could also be seen when comparing the luminescence of the aromatic adsorbate molecules. In all cases the luminescence was quenched on graphene. Molecule **4**, 6-amino-4-hydroxynaphthalene-2-sulfonic acid, has a well-defined pH dependant luminescence behaviour.[36] The molecule exhibits several emission bands, including bands at 405 nm and 435 nm, which could be used to monitor the pH dependence. Figure 11 shows how luminescence at 405 nm increases upon the deprotonation of its functional groups, first around the pK_a of the NH_3^+/NH_2 group at pH 3-4 and then at pH 10 corresponding to the pK_a of the OH/O^- group. With a free molecule, luminescence at 435 nm increases upon deprotonation of the NH_3^+ group but decreases when the OH group is deprotonated. When the molecule is adsorbed on graphene, the interaction between graphene and the molecule significantly changes the luminescence behaviour, especially by pushing the deprotonation of the OH group several pH-units further into the alkaline range. This implies significant interactions between the oxygen group and the graphene sheet, which act as an electron acceptor and donor, respectively. Because naphthalene has a relatively small aromatic structure, the π-π interactions between graphene and the molecule are weak, highlighting the role of the OH group as a binder between the molecule and graphene. Specifically, this demonstrates a relatively rare occasion, in which the interaction of a molecule with the graphene surface could be experimentally observed and attributed to a chemically specific process.

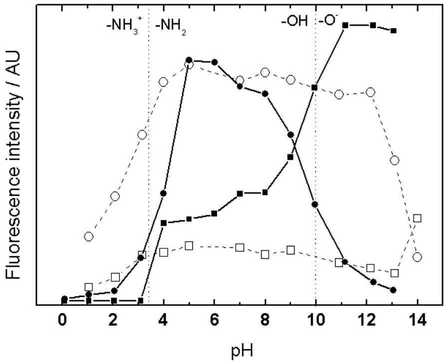

Figure 11. Comparison of luminescence intensities at 405 nm (solid square) and 435 nm (solid sphere) of free compound **4** and composite **G-4** (hollow square and sphere) as a function of pH. [Paper I]

These composite materials show similar properties to other graphene/adsorbate composites, including similar concentration and stability as well as quenched luminescence and other interactions between the adsorbate and graphene. The new adsorbates widen the range of suitable solubilisers for graphene even further and, therefore, allow better tailoring of possible applications.

4.2. Chemical Reduction of GO with Vanadium (III) and (IV)

Although the mechanical preparation methods for graphene materials are getting a foothold, they are still less used than chemical routes using graphene oxide. GO can be produced in large amounts using a multiple of relatively dangerous reaction routes and GO is probably a more versatile material to use. It can be dried and further redispersed, spin coated, sprayed or printed on surfaces, and is soluble in several polar solvents. The chemical reduction of GO is the dominant method and hydrazine is the most popular but not the most efficient reducing agent for GO. The properties of hydrazine-reduced GO are good enough for many applications, which, along with the tradition and all the available research data, explains its popularity. New reducing agents with as good or higher reduction efficiency are constantly reported but most of them have some limitations. One of the other reducing agents is vanadium in its V(III) and V(IV) oxidation levels. As a matter of fact, V(II) would be an even better reductant but it is highly reactive, which makes its use for GO reduction difficult. We found that vanadium(III) is as efficient a reducing agent as hydrazine [Paper II], but will not probably widely replace this toxic and explosive reductant because it is somewhat toxic heavy metal compound itself. What makes vanadium desirable is that it may be combined with energy storage devices, such as redox flow batteries[124], lithium ion batteries[125,126], where it has already been used together with graphene sheets.

After an accidental discovery of the reduction capability of VCl_3 we run a series of experiments in order to understand and test its effect. It was found out that 1.0 mg/ml aqueous GO solution could be reduced with millimolar scale VCl_3 concentrations at temperatures close to 100 °C within 45 minutes. Exposing the GO solution to 20 mM VCl_3 showed that the reduction took place already at only slightly elevated temperatures (Fig 12.) The XPS results indicate that the most significant oxygen functionality loss occurs around 35 °C and slowly reaches a stable level around 80-100 °C. Figure 12b displays the detailed C 1s spectrum of a GO sample reduced at 95 °C, showing a dominant C=C/C-C peak but a still clearly visible C-O peak. The C/O atomic ratio for this material was measured to be 4.0 compared to 2.3 of GO. Conductivity measurements of the GO films reduced under similar conditions proved also the recovery of the aromatic network of GO at low temperatures, although at slightly higher than indicated by the XPS measurements. This could be explained by the difference in the sample geometry, which was a packed film on a substrate in the former and an aqueous dispersion with large surface area in the latter. In addition, vanadium was almost completely removed from RGO after washing. Only about 0.005 vanadium atoms were left behind per one carbon atom, the only vanadium species seen in the XPS spectra being vanadium pentoxide, V_2O_5. The UV-Vis measurements revealed that the reaction solution contained predominantly V(IV) and V(V) species after the reduction. During the reduction V(III) turns quite rapidly into V(IV), which then slowly disproportionates to V(III) and V(V).

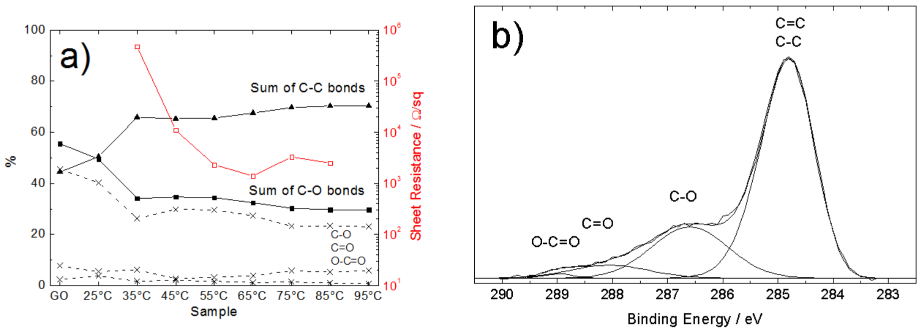

Figure 12. Relative fractions of total carbons based on XPS measurements of RGO samples reduced with V(III) at different temperatures (a). XPS C 1s spectrum of RGO reduced with 20 mM V(III) at 95°C. [Paper II]

The redox potential of V(III)/V(IV) pair should not be cathodic enough, compared to electrochemical measurements, to reduce GO under the conditions used. However, GO is well reduced upon exposure to V(III). A strong tendency of vanadium, especially V(IV) and V(V) species, to form oxygen complexes is in key role in the reaction between vanadium ions and GO. In addition, the reported reduction potentials for GO vary widely in literature and the generally used highly cathodic potentials in the electrochemical reduction of GO may represent a high cathodic overpotential required and not the thermodynamic redox potentials involved in reduction. However, more mysterious is the reduction by V(IV), which is not a reducing agent at all. As described above, V(IV) was slowly turning into V(V) during the reduction. This V(V) generation takes place via the disproportionation reaction of V(IV), in which reaction both V(V) and V(III) are created. The reaction equilibrium is highly unfavourable for this reaction, but the reaction of the V(III) with GO probably drives the reaction.

In order to compare V(III) with other a reducing agents we chose hydrazine as “the standard reducing agent”, and Ti(III), which has similar properties to V(III), including the formal redox potential of the Ti(IV)/Ti(III) pair. All these reducing agents were used under the same reaction conditions as V(III), i.e., 20 mM aqueous solution, 45 min reduction time at 95 °C. Titanium trichloride has been used in several publications to reduce GO quite efficiently to RGO. The most significant difference between Ti(III) and V(III) is that titanium forms insoluble oxides, therefore, creating RGO/TiO_2 composites, whereas vanadium oxides are all generally soluble in water. This difference could be seen already with a naked eye: V(III)-reduced GO had shiny metallic surface while Ti(III)-reduced GO was covered with a thick white TiO_2 layer and, even after extensive washing, TiO_2 was not fully removed as seen by AFM. In the AFM image, spherical TiO_2 particles decorate the whole film (Fig. 13d).

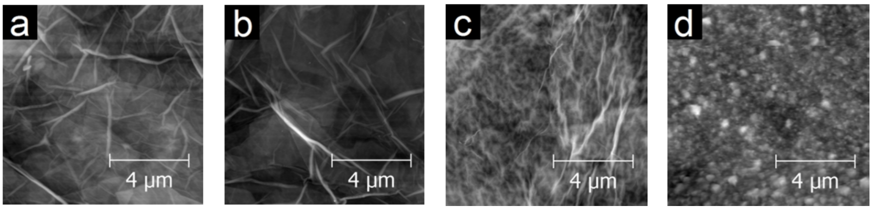

Figure 13. AFM images from (a) GO film, (b) V(III), (d) Ti(III) and (c) hydrazine –reduced GO films. [Paper II]

The AFM images reveal that the surface of the V(III)-reduced GO is hardly changed, compared to original GO. The hydrazine reduced GO shows small-scale wrinkles but is otherwise similar to the GO film. The RGO films reduced with V(III) and hydrazine exhibited conductivity of the same order of magnitude and also similar C/O atomic ratio. Upon comparison of the XPS results, especially C 1s spectra of the three reduced materials, it can be noted that samples reduced with Ti(III) and V(III) are almost identical, consisting approximately of 70 % carbon-carbon and 30 % carbon-oxygen moieties. Hydrazine reduced GO, on the other hand, has carbon species distribution of 73.5 % carbon-carbon, 14 % carbon-oxygen and 12.5 % carbon-nitrogen moieties. This indicates a better removal of oxygen from hydrazine reduced GO but also a strong functionalization with nitrogen. In short, despite its unknown reduction mechanism, V(III) is an efficient reducing agent, and under mild temperatures and low concentrations it is as efficient as Ti(III) and hydrazine. V(III) leaves only trace amounts of V_2O_5 in RGO and in many applications these amounts can be neglected. Although V(III) may not be the best reducing agent for GO, it achieves good enough reduction, comparable to hydrazine, and opens up new possibilities, especially for energy storage devices.

4.3. Electrochemical Reduction of GO

When graphene oxide is subjected to large enough cathodic potential in an electrochemical system, it undergoes an irreversible reduction. Similar changes in colour and spectral characteristics and an increase in conductivity can be observed both in electrochemically reduced GO and in RGO reduced by other means.[Paper IV] In cyclic voltammetric experiments typically a single reduction peak can be seen. For thin GO films this peak is observed only at the first cycle as the whole film is reduced during the single cathodic sweep. The reduction potential of GO is dependent on solvent or pH of an aqueous solution. In neutral aqueous solutions the reduction starts at ca. -0.8 V (vs. Ag/AgCl) and shifts towards more or less cathodic potentials with higher or lower pH, respectively (Fig. 14).[Paper III and IV] The change of pH could also have some effect on the structure of GO itself. Especially highly basic environment promotes the breaking of some of the functional groups in graphene oxide or cause the removal of the oxidation debris. This generally requires highly basic conditions and elevated temperature [73,74] or prolonged reaction time[80].

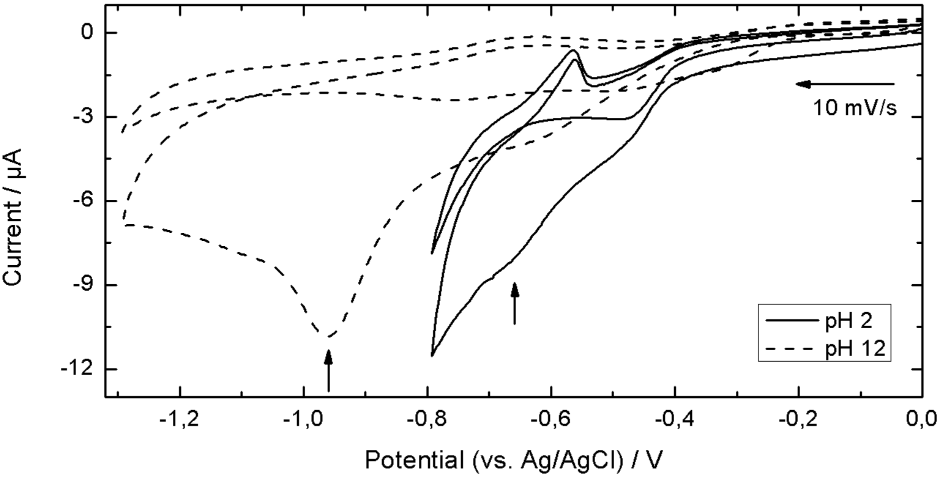

Figure 14. Cyclic voltammograms of the GO reduction (first two cycles) at pH 2 and 12. Scan direction and the main reduction peaks of GO are indicated with arrows. (Conditions: 0.1 M aqueous phosphate buffer, working electrode a fluorine doped tin oxide glass) [Paper IV]

In situ spectroelectrochemical measurements are a valuable tool for monitoring changes in spectra during electrochemical processes. In aqueous solutions at neutral pH, the electrochemical reduction of GO was monitored in situ with the SEIRAS and SERS techniques [Paper III]. In the SEIRAS measurements, an increase in intensity of the C=C vibration band and changes in the OH group vibrations took place after -0.8 V, whereas no significant changes occurred at less cathodic potentials. *In situ* SERS measurements followed the same trend than SEIRAS, showing that the shift of the G band towards lower wavenumbers, which is related to the restoration of the aromatic network, took place in the same potential range. Similar changes in the G band position has been reported earlier for GO reduced chemically, electrochemically and thermally.[127-129]

High pH values in aqueous solution shift the potential window and the reduction peak towards more cathodic potentials but, at the same time, allow a more effective reduction than at lower pH. [Paper IV] Upon reduction of GO at potentials corresponding to the reduction peak in voltammograms at either pH 2 or 12 (i.e., close to -0.8 V or -1.5 V vs. Ag/AgCl, respectively), some differences can be seen in the IR spectra. In the IR spectrum of GO reduced at -0.8 V at pH 2, oxygen-containing functional groups, such as ketonic and hydroxyl groups, are still clearly seen. If the reduction takes place at pH 12 the features attributed to these same groups are less evident and the spectrum begins to resemble the featureless IR spectrum of graphene. Only the C=C and some hydroxyl related vibrations are left in the spectrum. The elemental analysis performed with EDX indicates that GO (C/O ratio of 1.37) is reduced further at the more cathodic potentials required at pH 12 (C/O = 4.10) than at those potentials used at pH 2 (C/O = 3.37).

The potential window can only be manipulated within certain limits in aqueous solutions, while certain organic solvents provide significantly larger potential windows. Examples of such solvents are, e.g., acetonitrile (AN), tetrahydrofuran (THF) and propylene carbonate (PC), in which potentials close to -3.0 V vs. Fc/Fc^+ can be achieved. At these extreme potentials some problems were encountered, including the stability of the transparent fluorine doped tin oxide working electrode in acetonitrile [Paper IV] and side reactions of tetrahydrofuran and the electrolyte salt [Paper V]. Nevertheless, GO behaved similarly in CV measurements in all these organic solvents as in aqueous solutions, exhibiting a single peak during the first cathodic potential sweep. The reduction peaks for the GO films on gold were in the range between -1.9 and -2.3 V (vs. Fc/Fc^+), the least and most cathodic values referring to acetonitrile and propylene carbonate, respectively.[Paper V]

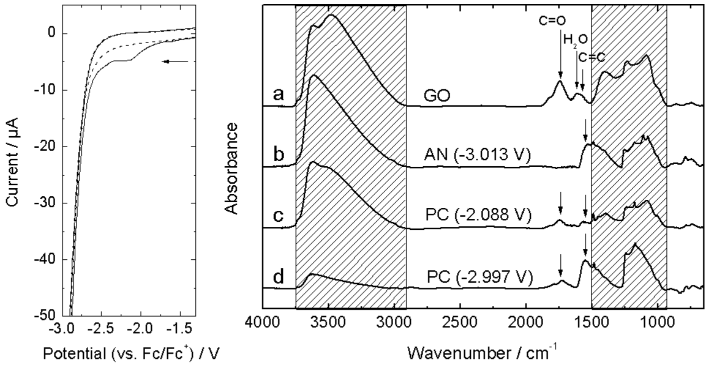

Figure 15. Left; cyclic voltammograms of the reduction of a monolayer of GO (solid line) and the bare electrode (dashed line). An arrow indicates the scan direction at 50 mV/s scanning rate. (Conditions: 0.1 M tetraethylammonium tetrafluorophosphate in PC, working electrode fluorine doped tin oxide glass) Right; the IR spectra of GO and reduced GO in AN and PC, with the corresponding reduction potentials (vs. Fc/Fc^+). Arrows indicate peaks attributed to the groups shown in the figure.[Paper IV]

Ex situ IR measurements of GO films reduced in PC at the potential of the reduction peak and at -3.0 V (vs. Fc/Fc^+) indicate that changes continue after the reduction peak in the voltammogram. In the spectra (Fig. 15), the C=C vibration began to dominate over the vibrations attributable to, e.g., the OH and C=O groups. The strong C=C band was also present in the spectra of GO reduced in acetonitrile at the highest cathodic potential possible. Furthermore, a significantly weaker signature of intercalated water is seen in the RGO films reduced in organic solvents than in those reduced in aqueous solutions.

In order to obtain deeper insight into the reduction process, *in situ* measurements were introduced also in organic solvents.[Paper V] AN, PC and THF were selected as solvents due to their wide electrochemical potential windows, especially at the cathodic side. Acetonitrile interfered less than the other two solvents with the spectroscopic measurements and enabled an excellent monitoring of the spectral changes of GO. In the CV of GO in acetonitrile, the reduction peak was observed at -1.86 V with the onset potential at ca. -1.25 V (vs. Fc/Fc^+). A small prepeak was seen at ca. -1 V but its origin could not be reliably assigned to GO. The overall Faradaic current started slowly to grow around -0.8 V. For *in situ* Raman measurements two instruments were used for comparison, a FT-Raman with NIR excitation at 1064 nm for SERS and a dispersive Raman with excitation at 514 nm for normal Raman spectroscopy. In the SERS measurements a self-assembled GO monolayer was used instead of a thin film. The main focus was on the changes of the G band position. In both measurements, a clear evidence of a downshift of the G band between -0.5 and -1.0 V (vs. Fc/Fc^+) can be seen. (Fig. 16) The G band then stabilises between -1.0 and -1.5 V in both cases. This observed downshift is irreversible indicating permanent structural changes in GO during these reduction potentials. In the case of thicker GO film (λ_{ex} = 514 nm), the downshift continues at more extreme cathodic potentials. This change is, however, reversible and, at open circuit or upon switching the potential back to the initial value, the G band shifts back to the same position it was after the initial irreversible decrease in wavenumber. For this reason only the irreversible change can be related to structural changes, mainly restoration of C=C bonds, in GO. The difference in G band changes between the two measurements might be caused by different measurement techniques, or by the apparent peak position changes due to the wavelength dependant D' band lying underneath the G band.

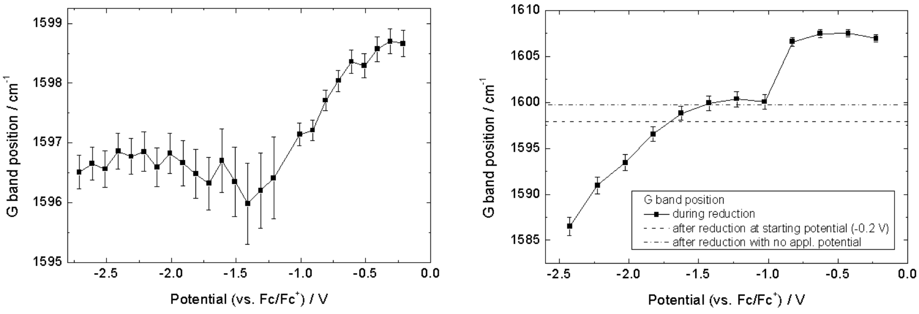

Figure 16. G band position changes during *in situ* electrochemical reduction of GO in acetonitrile. SERS (left) measurements (FT-Raman, λ_{ex} = 1064 nm) on a single layer GO and dispersive (right) Raman measurements (λ_{ex} = 514 nm) on thin GO film. (Conditions: 0.1 M $LiPF_6$ in acetonitrile, working electrode: Au) [Paper V]

CV and *in situ* Raman measurements of GO monolayer in propylene carbonate showed two stages at GO reduction. In the voltammogram (Fig. 17) Faradaic current increases between -1.0 and -1.5 V (vs.

Fc/Fc$^+$) peaking at -1.54 V. There is also second peak at -2.7 V with a shoulder at -2.2 V. The SERS measurements of the GO monolayer show also two different phases for the G band around the same potentials (Fig. 17). In SERS, the first downshift of G band starts around -0.7 V and levels between -1.2 and -1.7 V. The second downshift takes place at -1.8 V and levels after -2.0 V. The first reduction peak in CV and the shoulder in second peak correspond to the changes seen in G band, although the potentials in CV are shifted to more cathodic due to kinetic nature of CV versus steady potentials in Raman. These observed G band position changes are irreversible as were the changes in AN. The second peak in CV and the reversible changes after -2.5 V in G band position are unrelated to the reduction of GO.

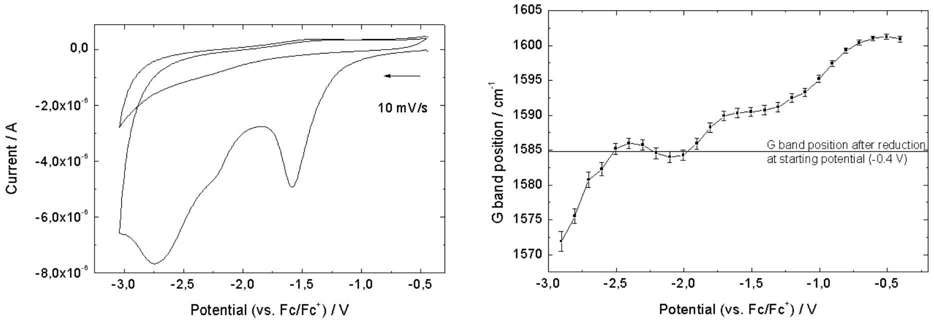

Figure 17. CV of monolayer GO (first and second cycle) on the left. (Conditions: 0.1 M $LiPF_6$ in PC, working electrode Au.) G band position changes in SERS measurements during *in situ* electrochemical reduction of GO monolayer in PC.

In situ IR experiment in AN shows significant changes in the vibration bands corresponding to the C-OH groups above 3000 cm^{-1}, the C=O groups at 1750 and 1820 cm^{-1} and the C=C at 1579 cm^{-1}. (Fig. 18) The greatest changes occurred around -1.3 V (vs. Fc/Fc$^+$), and they level off before -2.0 V. At potentials less cathodic than -1.0 V the spectral changes are weaker, although they started around -0.5 V. During the electrochemical reduction of GO, a C=C related band shows a significant increase indicating the restoration of the aromatic graphene structure. At the same time, the intensity of vibrations belonging to keto groups decrease. The C-OH groups in GO show changes as the band of closely located OH groups at 3370 cm^{-1} is decreasing and band corresponding to isolated OH groups at 3610 cm^{-1} is increased.[95] This also clearly indicates the removal of oxygen-containing groups from the material. The spectral region below 1500 cm^{-1} contains multiple closely located OH and C-O vibrations and some vibrations from electrolyte, making this region too complicated to be analysed in detail.

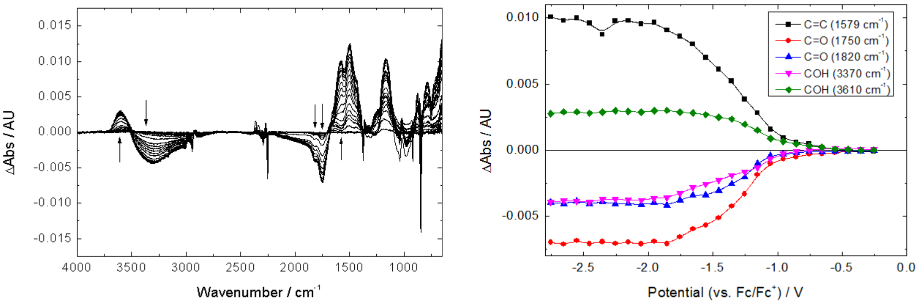

Figure 18. *In situ* FTIR spectral changes during electrochemical reduction of GO film in acetonitrile, compared to the spectrum at starting potential of -0.225 V (vs. Fc/Fc$^+$). The changes in the intensity of the various functional groups as well as C=C vibration are plotted as function of applied potential. (Conditions: 0.1 M $LiPF_6$ in acetonitrile, working electrode: Au) [Paper V]

Reduction of GO in THF resembled that of a reduction in acetonitrile. The G band shifts towards smaller wavenumbers and levels off before -1.2 V (vs. Fc/Fc$^+$), after which the electrolyte instability at more cathodic potentials complicate the interpretation of the results. In situ infrared measurements were also very similar to changes in acetonitrile. In summary, in situ Raman and IR measurements showed that GO film undergoes an irreversible change during the electrochemical reduction in all investigated organic solvents. The changes in G band mainly correspond to structural recovery of aromatic network, but also reflect the changes occurring near the aromatic domains. In IR, the removal of various functional groups can be seen taking place, with no clear evidence between the evolutions of various functional groups during the reduction. Simultaneously to the removal of the functional groups, the recovery of aromatic carbon structures can be seen. Because the irreversible changes occurred within the potential window of the solvents, the required potentials for the reduction of GO film in these solvents could be estimated from the IR and Raman results. The changes in spectroscopies could also be, to some extent, linked to the reduction processes seen in CV measurements.

Based on the electrochemical experiments, GO can easily be reduced in various organic solvents or in aqueous solutions. The reduction potentials, at which the reduction starts, are dependent on the medium but in all cases, the more cathodic the used reduction potential the better the reduction as was seen in Paper IV. This is especially true for aqueous solutions, which have a limited electrochemical potential window. On the other hand, in organic solvents a limiting potential for the reduction can be reached, after which no irreversible changes occur in the spectra. Electrochemistry offers an interesting alternative to GO reduction, which could be especially useful in applications, such as solar cells and chemical sensors, in which conductive polymers can be polymerised and GO reduced, both electrochemically.

5. Conclusions

In this work, existing techniques, together with a few new or modified methods, were used to prepare graphene based materials. A mechanical exfoliation technique with novel adsorbate molecules was used to prepare water-soluble graphene/adsorbate-composites. Strong π-π –interactions as well as donor/acceptor-interactions played a key role in the success of the adsorbates to solubilise graphene sheets.

Graphene oxide is a common starting point for graphene based materials and it is usually reduced with reducing agents, such as hydrazine, in order to recover the aromatic structure. In this work, we discovered that vanadium at oxidation states III and IV was able to reduce GO, despite that V(III) is a rather weak reducing agent and V(IV) is not a reducing agent at all. This was attributed to the strong affinity of vanadium(III) towards oxygen and, in case of V(IV), to its disproportionation reaction. The reduction using vanadium(III) was efficient already at mild temperatures and the RGO formed was comparable to that reduced using hydrazine or Ti(III).

Spectroelectrochemical investigations on the GO reduction showed that it is a complex process. Electrochemical reduction can be achieved easily in aqueous solutions but also in some organic solvents. The required reduction potential depends on environment and can be manipulated, e.g., by pH in aqueous solutions. The in situ spectroelectrochemical measurements were able to link the spectral changes in the Raman and infrared spectra to the observed electrochemical behaviour.

This Thesis brings new information about the chemical and electrochemical methods for the graphene oxide reduction, as well as broadens the adsorbate selection for mechanically exfoliated graphenes and gives insight into the adsorbate-graphene interactions.

References

[1] A Bianco, H Cheng, T Enoki, Y Gogotsi, RH Hurt, N Koratkar, et al. All in the graphene family – A recommended nomenclature for two-dimensional carbon materials, Carbon. 65 (2013) 1-6.

[2] S Bae, H Kim, Y Lee, X Xu, J Park, Y Zheng, et al. Roll-to-roll production of 30-inch graphene films for transparent electrodes, Nat Nano. 5 (2010) 574-578.

[3] K Novoselov, A Geim, S Morozov, D Jiang, Y Zhang, S Dubonos, et al. Electric field effect in atomically thin carbon films, Science. 306 (2004) 666-669.

[4] M Liu, VI Artyukhov, H Lee, F Xu, BI Yakobson. Carbyne from First Principles: Chain of C Atoms, a Nanorod or a Nanorope, ACS Nano. 7 (2013) 10075-10082.

[5] C Lee, X Wei, JW Kysar, J Hone. Measurement of the Elastic Properties and Intrinsic Strength of Monolayer Graphene, Science. 321 (2008) 385-388.

[6] KS Kim, Y Zhao, H Jang, SY Lee, JM Kim, KS Kim, et al. Large-scale pattern growth of graphene films for stretchable transparent electrodes, Nature. 457 (2009) 706-710.

[7] JR Potts, DR Dreyer, CW Bielawski, RS Ruoff. Graphene-based polymer nanocomposites, Polymer. 52 (2011) 5-25.

[8] DDL Chung. Review Graphite, J.Mater.Sci. 37 (2002) 1475-1489.

[9] K Novoselov, A Geim, S Morozov, D Jiang, M Katsnelson, I Grigorieva, et al. Two-dimensional gas of massless Dirac fermions in graphene, Nature. 438 (2005) 197-200.

[10] RR Nair, P Blake, AN Grigorenko, KS Novoselov, TJ Booth, T Stauber, et al., Fine Structure Constant Defines Visual Transparency of Graphene, Science. 320 (2008) 1308-1308.

[11] A Bianco. Graphene: Safe or Toxic? The Two Faces of the Medal, Angewandte Chemie International Edition. 52 (2013) 4986-4997.

[12] VC Sanchez, A Jachak, RH Hurt, AB Kane. Biological Interactions of Graphene-Family Nanomaterials: An Interdisciplinary Review, Chem.Res.Toxicol. 25 (2012) 15-34.

[13] AB Seabra, AJ Paula, R de Lima, OL Alves, N Durán. Nanotoxicity of Graphene and Graphene Oxide, Chem.Res.Toxicol. 27 (2014) 159-168.

[14] AM Jastrzębska, P Kurtycz, AR Olszyna. Recent advances in graphene family materials toxicity investigations, Journal of Nanoparticle Research. 14 (2012) 1320.

[15] A Schinwald, FA Murphy, A Jones, W MacNee, K Donaldson. Graphene-Based Nanoplatelets: A New Risk to the Respiratory System as a Consequence of Their Unusual Aerodynamic Properties, ACS Nano. 6 (2012) 736-746.

[16] MC Duch, GRS Budinger, YT Liang, S Soberanes, D Urich, SE Chiarella, et al. Minimizing Oxidation and Stable Nanoscale Dispersion Improves the Biocompatibility of Graphene in the Lung, Nano Lett. 11 (2011) 5201-5207.

[17] H Yue, W Wei, Z Yue, B Wang, N Luo, Y Gao, et al. The role of the lateral dimension of graphene oxide in the regulation of cellular responses, Biomaterials. 33 (2012) 4013-4021.

[18] T Kobayashi, M Bando, N Kimura, K Shimizu, K Kadono, N Umezu, et al. Production of a 100-m-long high-quality graphene transparent conductive film by roll-to-roll chemical vapor deposition and transfer process, Appl.Phys.Lett. 102 (2013) 023112.

[19] L Chen, Y Hernandez, X Feng, K Müllen. From Nanographene and Graphene Nanoribbons to Graphene Sheets: Chemical Synthesis, Angewandte Chemie International Edition. 51 (2012) 7640-7654.

[20] KR Paton, E Varrla, C Backes, RJ Smith, U Khan, A O'Neill, et al. Scalable production of large quantities of defect-free few-layer graphene by shear exfoliation in liquids, Nat Mater. 13 (2014) 624-630.

[21] C Shih, A Vijayaraghavan, R Krishnan, R Sharma, J Han, M Ham, et al. Bi- and trilayer graphene solutions, Nat Nano. 6 (2011) 439-445.

[22] Y Hernandez, V Nicolosi, M Lotya, FM Blighe, Z Sun, S De, et al. High-yield production of graphene by liquid-phase exfoliation of graphite, Nat Nano. 3 (2008) 563-568.

[23] Y Hernandez, M Lotya, D Rickard, SD Bergin, JN Coleman. Measurement of Multicomponent Solubility Parameters for Graphene Facilitates Solvent Discovery, Langmuir. 26 (2010) 3208-3213.

[24] J Texter. Graphene dispersions, Current Opinion in Colloid & Interface Science. 19 (2014) 163-174.

[25] U Khan, A O'Neill, M Lotya, S De, JN Coleman. High-Concentration Solvent Exfoliation of Graphene, Small. 6 (2010) 864-871.

[26] AB Bourlinos, V Georgakilas, R Zboril, TA Steriotis, AK Stubos. Liquid-Phase Exfoliation of Graphite Towards Solubilized Graphenes, Small. 5 (2009) 1841-1845.

[27] D Nuvoli, V Alzari, R Sanna, S Scognamillo, M Piccinini, L Peponi, et al. The production of concentrated dispersions of few-layer graphene by the direct exfoliation of graphite in organosilanes, Nanoscale Research Letters. 7 (2012) 674.

[28] U Khan, H Porwal, A O'Neill, K Nawaz, P May, JN Coleman. Solvent-Exfoliated Graphene at Extremely High Concentration, Langmuir. 27 (2011) 9077-9082.

[29] A O'Neill, U Khan, PN Nirmalraj, J Boland, JN Coleman. Graphene Dispersion and Exfoliation in Low Boiling Point Solvents, J.Phys.Chem.C. 115 (2011) 5422-5428.

[30] X Chen, JF Dobson, CL Raston. Vortex fluidic exfoliation of graphite and boron nitride, Chem.Commun. 48 (2012) 3703-3705.

[31] S Bose, T Kuila, AK Mishra, NH Kim, JH Lee. Preparation of non-covalently functionalized graphene using 9-anthracene carboxylic acid, Nanotechnology. 22 (2011) 405603.

[32] D Parviz, S Das, HST Ahmed, F Irin, S Bhattacharia, MJ Green. Dispersions of Non-Covalently Functionalized Graphene with Minimal Stabilizer, ACS Nano. 6 (2012) 8857-8867.

[33] H Yang, Y Hernandez, A Schlierf, A Felten, A Eckmann, S Johal, et al. A simple method for graphene production based on exfoliation of graphite in water using 1-pyrenesulfonic acid sodium salt, Carbon. 53 (2013) 357-365.

[34] M Lotya, PJ King, U Khan, S De, JN Coleman. High-Concentration, Surfactant-Stabilized Graphene Dispersions, ACS Nano. 4 (2010) 3155-3162.

[35] Z Sun, J Masa, Z Liu, W Schuhmann, M Muhler. Highly Concentrated Aqueous Dispersions of Graphene Exfoliated by Sodium Taurodeoxycholate: Dispersion Behavior and Potential Application as a Catalyst Support for the Oxygen-Reduction Reaction, Chemistry - A European Journal. 18 (2012) 6972-6978.

[36] H Paloniemi, T Ääritalo, T Laiho, H Liuke, N Kocharova, K Haapakka, et al. Water-Soluble Full-Length Single-Wall Carbon Nanotube Polyelectrolytes: Preparation and Characterization, J Phys Chem B. 109 (2005) 8634-8642.

[37] A Schlierf, H Yang, E Gebremedhn, E Treossi, L Ortolani, L Chen, et al. Nanoscale insight into the exfoliation mechanism of graphene with organic dyes: effect of charge, dipole and molecular structure, Nanoscale. 5 (2013) 4205-4216.

[38] RJ Smith, M Lotya, JN Coleman. The importance of repulsive potential barriers for the dispersion of graphene using surfactants, New J.Phys. 12 (2010) 125008.

[39] AS Wajid, S Das, F Irin, HST Ahmed, JL Shelburne, D Parviz, et al. Polymer-stabilized graphene dispersions at high concentrations in organic solvents for composite production, Carbon. 50 (2012) 526-534.

[40] AB Bourlinos, V Georgakilas, R Zboril, TA Steriotis, AK Stubos, C Trapalis. Aqueous-phase exfoliation of graphite in the presence of polyvinylpyrrolidone for the production of water-soluble graphenes, Solid State Commun. 149 (2009) 2172-2176.

[41] MS Kang, KT Kim, JU Lee, WH Jo. Direct exfoliation of graphite using a non-ionic polymer surfactant for fabrication of transparent and conductive graphene films, J.Mater.Chem.C. 1 (2013) 1870-1875.

[42] A Griffith, SM Notley. pH dependent stability of aqueous suspensions of graphene with adsorbed weakly ionisable cationic polyelectrolyte, J.Colloid Interface Sci. 369 (2012) 210-215.

[43] JT Seo, AA Green, AL Antaris, MC Hersam. High-Concentration Aqueous Dispersions of Graphene Using Nonionic, Biocompatible Block Copolymers, J.Phys.Chem.Lett. 2 (2011) 1004-1008.

[44] SM Notley. Highly Concentrated Aqueous Suspensions of Graphene through Ultrasonic Exfoliation with Continuous Surfactant Addition, Langmuir. 28 (2012) 14110-14113.

[45] M Lotya, Y Hernandez, PJ King, RJ Smith, V Nicolosi, LS Karlsson, et al. Liquid Phase Production of Graphene by Exfoliation of Graphite in Surfactant/Water Solutions, J.Am.Chem.Soc. 131 (2009) 3611-3620.

[46] C Shih, GLC Paulus, QH Wang, Z Jin, D Blankschtein, MS Strano. Understanding Surfactant/Graphene Interactions Using a Graphene Field Effect Transistor: Relating Molecular Structure to Hysteresis and Carrier Mobility, Langmuir. 28 (2012) 8579-8586.

[47] Q Su, S Pang, V Alijani, C Li, X Feng, K Müllen. Composites of Graphene with Large Aromatic Molecules, Adv Mater. 21 (2009) 3191-3195.

[48] U Khan, A O'Neill, H Porwal, P May, K Nawaz, JN Coleman. Size selection of dispersed, exfoliated graphene flakes by controlled centrifugation, Carbon. 50 (2012) 470-475.

[49] AA Green, MC Hersam. Solution Phase Production of Graphene with Controlled Thickness via Density Differentiation, Nano Lett. 9 (2009) 4031-4036.

[50] BC Brodie. On the Atomic Weight of Graphite, Philosophical Transactions of the Royal Society of London. 149 (1859) 249-259.

[51] L Staudenmaier. Verfahren zur Darstellung der Graphitsäure, Berichte der deutschen chemischen Gesellschaft. 31 (1898) 1481-1487.

[52] U Hofmann, E König. Untersuchungen über Graphitoxyd, Zeitschrift für anorganische und allgemeine Chemie. 234 (1937) 311-336.

[53] W Hummers, R Offeman. Preparation of Graphitic Oxide, J.Am.Chem.Soc. 80 (1958) 1339-1339.

[54] DC Marcano, DV Kosynkin, JM Berlin, A Sinitskii, Z Sun, A Slesarev, et al. Improved Synthesis of Graphene Oxide, ACS Nano. 4 (2010) 4806-4814.

[55] AYS Eng, A Ambrosi, CK Chua, F Šaněk, Z Sofer, M Pumera. Unusual Inherent Electrochemistry of Graphene Oxides Prepared Using Permanganate Oxidants, Chemistry - A European Journal. 19 (2013) 12673-12683.

[56] CK Chua, Z Sofer, M Pumera. Graphite Oxides: Effects of Permanganate and Chlorate Oxidants on the Oxygen Composition, Chemistry - A European Journal. 18 (2012) 13453-13459.

[57] S You, SM Luzan, T Szabó, AV Talyzin. Effect of synthesis method on solvation and exfoliation of graphite oxide, Carbon. 52 (2013) 171-180.

[58] M Hirata, T Gotou, S Horiuchi, M Fujiwara, M Ohba. Thin-film particles of graphite oxide 1:: High-yield synthesis and flexibility of the particles, Carbon. 42 (2004) 2929-2937.

[59] HK Jeong, MH Jin, KP So, SC Lim, YH Lee. Tailoring the characteristics of graphite oxides by different oxidation times, J.Phys.D. 42 (2009) 065418.

[60] K Krishnamoorthy, M Veerapandian, K Yun, S- Kim. The chemical and structural analysis of graphene oxide with different degrees of oxidation, Carbon. 53 (2013) 38-49.

[61] D Kang, HS Shin. Control of size and physical properties of graphene oxide by changing the oxidation temperature, Carbon Letters. 13 (2012) 39-43.

[62] T Szabo, O Berkesi, P Forgo, K Josepovits, Y Sanakis, D Petridis, et al. Evolution of surface functional groups in a series of progressively oxidized graphite oxides, Chem.Mat. 18 (2006) 2740-2749.

[63] A Dimiev, DV Kosynkin, LB Alemany, P Chaguine, JM Tour. Pristine Graphite Oxide, J.Am.Chem.Soc. 134 (2012) 2815-2822.

[64] C Botas, P Álvarez, C Blanco, R Santamaría, M Granda, P Ares, et al. The effect of the parent graphite on the structure of graphene oxide, Carbon. 50 (2012) 275-282.

[65] U Hofmann, R Holst. Über die Säurenatur und die Methylierung von Graphitoxyd, Berichte der deutschen chemischen Gesellschaft (A and B Series). 72 (1939) 754-771.

[66] G Ruess. Über das Graphitoxyhydroxyd (Graphitoxyd), Monatshefte für Chemie und verwandte Teile anderer Wissenschaften. 76 (1947) 381-417.

[67] T Nakajima, A Mabuchi, R Hagiwara. A new structure model of graphite oxide, Carbon. 26 (1988) 357-361.

[68] T Nakajima, Y Matsuo. Formation process and structure of graphite oxide, Carbon. 32 (1994) 469-475.

[69] H He, T Riedl, A Lerf, J Klinowski. Solid-State NMR Studies of the Structure of Graphite Oxide, J.Phys.Chem. 100 (1996) 19954-19958.

[70] A Lerf, H He, T Riedl, M Forster, J Klinowski. 13C and 1H MAS NMR studies of graphite oxide and its chemically modified derivatives, Solid State Ionics. 101–103, Part 2 (1997) 857-862.

[71] A Lerf, H He, M Forster, J Klinowski. Structure of graphite oxide revisited, J. Phys. Chem. B. 102 (1998) 4477-4482.

[72] AM Dimiev, LB Alemany, JM Tour. Graphene Oxide. Origin of Acidity, Its Instability in Water, and a New Dynamic Structural Model, ACS Nano. 7 (2013) 576-588.

[73] JP Rourke, PA Pandey, JJ Moore, M Bates, IA Kinloch, RJ Young, et al. The Real Graphene Oxide Revealed: Stripping the Oxidative Debris from the Graphene-like Sheets, Angewandte Chemie International Edition. 50 (2011) 3173-3177.

[74] HR Thomas, SP Day, WE Woodruff, C Vallés, RJ Young, IA Kinloch, et al. Deoxygenation of Graphene Oxide: Reduction or Cleaning? Chem.Mater. 25 (2013) 3580-3588.

[75] HR Thomas, C Valles, RJ Young, IA Kinloch, NR Wilson, JP Rourke. Identifying the fluorescence of graphene oxide, J.Mater.Chem.C. 1 (2013) 338-342.

[76] RLD Whitby, VM Gun'ko, A Korobeinyk, R Busquets, AB Cundy, K Laszlo, et al. Driving Forces of Conformational Changes in Single-Layer Graphene Oxide, ACS Nano. 6 (2012) 3967-3973.

[77] X Li, X Yang, L Jia, X Ma, L Zhu. Carbonaceous debris that resided in graphene oxide/reduced graphene oxide profoundly affect their electrochemical behaviors, Electrochemistry Communications. 23 (2012) 94-97.

[78] A Bonanni, A Ambrosi, CK Chua, M Pumera. Oxidation Debris in Graphene Oxide Is Responsible for Its Inherent Electroactivity, ACS Nano. 8 (2014) 4197-4204.

[79] VR Coluci, DST Martinez, JG Honório, AF de Faria, DA Morales, MS Skaf, et al. Noncovalent Interaction with Graphene Oxide: The Crucial Role of Oxidative Debris, J.Phys.Chem.C. 118 (2014) 2187-2193.

[80] Z Guo, S Wang, G Wang, Z Niu, J Yang, W Wu. Effect of oxidation debris on spectroscopic and macroscopic properties of graphene oxide, Carbon. 76 (2014) 203-211.

[81] D Li, MB Mueller, S Gilje, RB Kaner, GG Wallace. Processable aqueous dispersions of graphene nanosheets, Nat.Nanotechnol. 3 (2008) 101-105.

[82] B Konkena, S Vasudevan. Understanding Aqueous Dispersibility of Graphene Oxide and Reduced Graphene Oxide through pKa Measurements, J.Phys.Chem.Lett. 3 (2012) 867-872.

[83] RR Nair, HA Wu, PN Jayaram, IV Grigorieva, AK Geim. Unimpeded Permeation of Water Through Helium-Leak–Tight Graphene-Based Membranes, Science. 335 (2012) 442-444.

[84] JI Paredes, S Villar-Rodil, A Martínez-Alonso, JMD Tascón. Graphene Oxide Dispersions in Organic Solvents, Langmuir. 24 (2008) 10560-10564.

[85] JW Suk, RD Piner, J An, RS Ruoff. Mechanical Properties of Monolayer Graphene Oxide, ACS Nano. 4 (2010) 6557-6564.

[86] S Eigler, C Dotzer, A Hirsch, M Enzelberger, P Müller. Formation and Decomposition of CO2 Intercalated Graphene Oxide, Chem.Mater. 24 (2012) 1276-1282.

[87] JE Kim, TH Han, SH Lee, JY Kim, CW Ahn, JM Yun, et al. Graphene Oxide Liquid Crystals, Angewandte Chemie International Edition. 50 (2011) 3043-3047.

[88] X Yang, C Guo, L Ji, Y Li, Y Tu. Liquid Crystalline and Shear-Induced Properties of an Aqueous Solution of Graphene Oxide Sheets, Langmuir. 29 (2013) 8103-8107.

[89] SK Cushing, M Li, F Huang, N Wu. Origin of Strong Excitation Wavelength Dependent Fluorescence of Graphene Oxide, ACS Nano. 8 (2014) 1002-1013.

[90] J Shang, L Ma, J Li, W Ai, T Yu, GG Gurzadyan. The Origin of Fluorescence from Graphene Oxide, Sci.Rep. 2 (2012) 792.

[91] DR Dreyer, S Park, CW Bielawski, RS Ruoff. The chemistry of graphene oxide, Chem.Soc.Rev. 39 (2010) 228-240.

[92] S Eigler, A Hirsch. Chemistry with Graphene and Graphene Oxide - Challenges for Synthetic Chemists, Angewandte Chemie International Edition. 53 (2014) 7720-7738.

[93] RS Edwards, KS Coleman. Graphene synthesis: relationship to applications, Nanoscale. 5 (2013) 38-51.

[94] CD Zangmeister. Preparation and Evaluation of Graphite Oxide Reduced at 220 °C, Chem.Mater. 22 (2010) 5625-5629.

[95] M Acik, G Lee, C Mattevi, A Pirkle, RM Wallace, M Chhowalla, et al. The Role of Oxygen during Thermal Reduction of Graphene Oxide Studied by Infrared Absorption Spectroscopy, J.Phys.Chem.C. 115 (2011) 19761-19781.

[96] D Yang, A Velamakanni, G Bozoklu, S Park, M Stoller, RD Piner, et al. Chemical analysis of graphene oxide films after heat and chemical treatments by X-ray photoelectron and Micro-Raman spectroscopy, Carbon. 47 (2009) 145-152.

[97] S Dubin, S Gilje, K Wang, VC Tung, K Cha, AS Hall, et al. A One-Step, Solvothermal Reduction Method for Producing Reduced Graphene Oxide Dispersions in Organic Solvents, ACS Nano. 4 (2010) 3845-3852.

[98] OC Compton, B Jain, DA Dikin, A Abouimrane, K Amine, ST Nguyen. Chemically Active Reduced Graphene Oxide with Tunable C/O Ratios, ACS Nano. 5 (2011) 4380-4391.

[99] CK Chua, M Pumera. Chemical reduction of graphene oxide: a synthetic chemistry viewpoint, Chem.Soc.Rev. 43 (2014) 291-312.

[100] S Park, Y Hu, JO Hwang, E Lee, LB Casabianca, W Cai, et al. Chemical structures of hydrazine-treated graphene oxide and generation of aromatic nitrogen doping, Nat.Commun. 3 (2012) 638.

[101] H Chen, MB Müller, KJ Gilmore, GG Wallace, D Li. Mechanically Strong, Electrically Conductive, and Biocompatible Graphene Paper, Adv Mater. 20 (2008) 3557-3561.

[102] S Park, K Lee, G Bozoklu, W Cai, ST Nguyen, RS Ruoff. Graphene Oxide Papers Modified by Divalent Ionsâ€”Enhancing Mechanical Properties via Chemical Cross-Linking, ACS Nano. 2 (2008) 572-578.

[103] Z Fan, W Kai, J Yan, T Wei, L Zhi, J Feng, et al. Facile Synthesis of Graphene Nanosheets via Fe Reduction of Exfoliated Graphite Oxide, ACS Nano. 5 (2011) 191-198.

[104] J Zhang, Z Xiong, XS Zhao. Graphene-metal-oxide composites for the degradation of dyes under visible light irradiation, J.Mater.Chem. 21 (2011) 3634-3640.

[105] Y Si, ET Samulski. Synthesis of water soluble graphene, Nano Lett. 8 (2008) 1679-1682.

[106] A Ambrosi, CK Chua, A Bonanni, M Pumera. Lithium Aluminum Hydride as Reducing Agent for Chemically Reduced Graphene Oxides, Chem.Mater. 24 (2012) 2292-2298.

[107] CK Chua, M Pumera. Selective Removal of Hydroxyl Groups from Graphene Oxide, Chem. Eur. J. 19 (2013) 2005-2011.

[108] M Zhou, Y Wang, Y Zhai, J Zhai, W Ren, F Wang, et al. Controlled Synthesis of Large-Area and Patterned Electrochemically Reduced Graphene Oxide Films, Chem. Eur. J. 15 (2009) 6116-6120.

[109] A Peigney, C Laurent, E Flahaut, RR Bacsa, A Rousset. Specific surface area of carbon nanotubes and bundles of carbon nanotubes, Carbon. 39 (2001) 507-514.

[110] A Österholm, T Lindfors, J Kauppila, P Damlin, C Kvarnström. Electrochemical incorporation of graphene oxide into conducting polymer films, Electrochim.Acta. 83 (2012) 463-470.

[111] T Lindfors, A Österholm, J Kauppila, M Pesonen. Electrochemical reduction of graphene oxide in electrically conducting poly(3,4-ethylenedioxythiophene) composite films, Electrochim.Acta. 110 (2013) 428-436.

[112] A Jorio, MS Dresselhaus, R Saito, G Dresselhaus, Raman Spectroscopy in Graphene Related Systems, 1st ed., Wiley-VCH, Weinheim, 2011.

[113] S Reich, C Thomsen. Raman spectroscopy of graphite, Philosophical Transactions of the Royal Society of London.Series A: Mathematical, Physical and Engineering Sciences. 362 (2004) 2271-2288.

[114] P Nemes-Incze, Z Osváth, K Kamarás, LP Biró. Anomalies in thickness measurements of graphene and few layer graphite crystals by tapping mode atomic force microscopy, Carbon. 46 (2008) 1435-1442.

[115] RP Vidano, DB Fischbach, LJ Willis, TM Loehr. Observation of Raman band shifting with excitation wavelength for carbons and graphites, Solid State Commun. 39 (1981) 341-344.

[116] M Bouša, O Frank, I Jirka, L Kavan. In situ Raman spectroelectrochemistry of graphene oxide, physica status solidi (b). 250 (2013) 2662-2667.

[117] Z Kominkova, M Kalbac. Extreme electrochemical doping of a graphene-polyelectrolyte heterostructure, RSC Adv. 4 (2014) 11311-11316.

[118] I Calizo, AA Balandin, W Bao, F Miao, CN Lau. Temperature Dependence of the Raman Spectra of Graphene and Graphene Multilayers, Nano Lett. 7 (2007) 2645-2649.

[119] W Cai, RD Piner, FJ Stadermann, S Park, MA Shaibat, Y Ishii, et al. Synthesis and Solid-State NMR Structural Characterization of 13C-Labeled Graphite Oxide, Science. 321 (2008) 1815-1817.

[120] P Gao, D Gosztola, LH Leung, MJ Weaver. Surface-enhanced Raman scattering at gold electrodes: dependence on electrochemical pretreatment conditions and comparisons with silver, Journal of Electroanalytical Chemistry and Interfacial Electrochemistry. 233 (1987) 211-222.

[121] NI Kovtyukhova, PJ Ollivier, BR Martin, TE Mallouk, SA Chizhik, EV Buzaneva, et al. Layer-by-Layer Assembly of Ultrathin Composite Films from Micron-Sized Graphite Oxide Sheets and Polycations, Chem.Mater. 11 (1999) 771-778.

[122] X Zhou, X Huang, X Qi, S Wu, C Xue, FYC Boey, et al. In Situ Synthesis of Metal Nanoparticles on Single-Layer Graphene Oxide and Reduced Graphene Oxide Surfaces, J.Phys.Chem.C. 113 (2009) 10842-10846.

[123] M Acik, G Lee, C Mattevi, M Chhowalla, K Cho, YJ Chabal. Unusual infrared-absorption mechanism in thermally reduced graphene oxide, Nat.Mater. 9 (2010) 840-845.

[124] Z González, C Botas, C Blanco, R Santamaría, M Granda, P Álvarez, et al. Graphite oxide-based graphene materials as positive electrodes in vanadium redox flow batteries, J.Power Sources. 241 (2013) 349-354.

[125] X Rui, J Zhu, D Sim, C Xu, Y Zeng, HH Hng, et al. Reduced graphene oxide supported highly porous V2O5 spheres as a high-power cathode material for lithium ion batteries, Nanoscale. 3 (2011) 4752-4758.

[126] Y Qian, A Vu, W Smyrl, A Stein. Facile Preparation and Electrochemical Properties of V2O5-Graphene Composite Films as Free-Standing Cathodes for Rechargeable Lithium Batteries, J.Electrochem.Soc. 159 (2012) A1135-A1140.

[127] S Stankovich, DA Dikin, RD Piner, KA Kohlhaas, A Kleinhammes, Y Jia, et al. Synthesis of graphene-based nanosheets via chemical reduction of exfoliated graphite oxide, Carbon. 45 (2007) 1558-1565.

[128] GK Ramesha, S Sampath. Electrochemical Reduction of Oriented Graphene Oxide Films: An in Situ Raman Spectroelectrochemical Study, J.Phys.Chem.C. 113 (2009) 7985-7989.

[129] KN Kudin, B Ozbas, HC Schniepp, RK Prud'homme, IA Aksay, R Car. Raman Spectra of Graphite Oxide and Functionalized Graphene Sheets, Nano Lett. 8 (2008) 36-41.